Radiat. Phys. Chem. Vol. 43, No. 1/2, pp. 105–127, 1994
Printed in Great Britain

0969-806X/94 $6.00 + 0.00
Pergamon Press Ltd

ATOMIC DISPLACEMENT AND TOTAL IONIZING DOSE DAMAGE IN SEMICONDUCTORS

D. BRÄUNIG and F. WULF
Hahn-Meitner-Institut Berlin GmbH, Glienickerstrasse 100, 14109 Berlin 39, Germany

1. INTRODUCTION

A high energy particle interacts with matter in different ways depending on its energy, mass charge state and the species it interacts with. Among other mechanisms the most important are:

- Elastic scattering;
- Inelastic scattering;
- Fission.

Electromagnetic quanta are treated similarly as their main effect is the generation of energetic electrons which in turn belong to the class of particles.

In space we have to deal with:

- Electrons and their associated bremsstrahlung;
- Protons;
- Heavy and high energetic ions;
- Neutrons;
- Electromagnetic radiation, directly from the Sun or from nuclear excitations.

All these contributions may produce damage to the semiconductor device according to one of the above mentioned mechanisms or by more than one. For instance, an energetic heavy ion can interact with the semiconductor material by ionization (interaction with shell electrons results in free electrons) at the beginning of its travel and after slowing down by displacement of lattice atoms (interaction with the nucleus). There is even a certain probability for exciting the nucleus, which in turn may release some secondaries acting in a similar way as mentioned before.

It is therefore a good practice to classify the damage contributions into *Displacement* and *Ionization*, the latter is often called *Total Ionizing Dose* or shorthand TID. As the dose rate in space never exceeds some mrad(Si)/s transient effects can realistically be omitted, but the fact of accelerated testing poses a severe problem on the interpretation of ground data compared to actual space conditions.

The shrinking size of semiconductor devices is the source of a different failure mode (Single Event Phenomena or SEP) when the active region is hit by a heavy ion. This will be covered in a separate chapter.

In the following portions of this chapter we deal with the basics of displacement and ionization damage on semiconductor materials and devices in order to get a qualitative and quantitative understanding of the mechanisms involved, which is a prerequisite to properly predict the operational lifetime of a certain device in a specified space environment.

2. DISPLACEMENT DAMAGE

2.1. Introduction

From a physical point of view the interaction of radiation with matter is characterized by the probability of creating a displaced atom that can change the material's parameter of the semiconductor, for instance the minority carrier lifetime as the most sensitive quantity. This is caused by the introduction of additional recombination centres induced by radiation. Unfortunately there is no direct correlation between the probability in terms of a cross-section and the amount of created active centres. This becomes intuitively evident if one realises that the most probably created defects—the vacancy and the interstitial—are unstable at room temperature and these defects are mobile and tend to create more complex defects, for instance divacancies, A-centres or clusters. In addition the formation of more complex defects depends on the mobility of these simple defects which in turn is a function of the charge state of, say, the vacancy. The charge state on the other hand depends on the energetic position of the Fermi level in the semiconductor and this can be varied by a number of means: doping, temperature, charge injection, etc. In this way there is a variety of interdependencies that makes a prediction quite complicated.

2.2. Basic concepts

The most simple case to be considered is a head-on collision where the lattice atom (mass M) is directly hit by the impinging particle of mass m and energy E_1. After this encounter the incoming particle has a kinetic energy T_1 (T for transferred)

$$T_1 = E_1 \cdot \left(\frac{(m - M)^2}{(m + M)^2} \right) \tag{1}$$

and the recoil energy of the struck atom is

$$T_{2\max} = 4 \cdot E_1 \cdot \left(\frac{m \cdot M}{(m + M)^2} \right) \tag{2}$$

or in the case of an impinging relativistic electron ($m_e \ll M$) this energy is

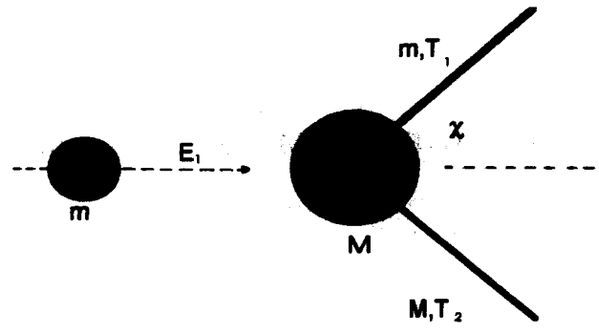

Fig. 1. Schematic representation of a collision event.

$$T_{2\max} = 2 \cdot E_1 \cdot \frac{m_e}{M}\left(2 + \frac{E_1}{m_e \cdot c^2}\right) \tag{3}$$

where m_e is the electron's rest mass ($m_e = 5.49 \cdot 10^{-4}$ amu) and c is the velocity of light ($m_e c^2 = 0.511$ MeV).

When the electron is scattered (angle χ), then the recoil energy becomes

$$T_2 = T_{2\max} \cdot \sin^2\left(\frac{\chi}{2}\right). \tag{4}$$

There is a certain amount of energy necessary to displace an atom from its lattice site, the displacement energy T_d, and this energy is in the range of 10–30 eV in the case of semiconductors. Consequently, a minimum energy $E_{1\min}$ of the incident particle is required, the so-called threshold energy E_{th}, for a displacement event. In the case of a relativistic electron and a maximum energy transfer to the lattice atom (head-on collision) this threshold energy is given by

$$E_{th} = E_{1\min} = m_e \cdot c^2 \cdot \left(\sqrt{1 + \frac{T_d}{2 \cdot m_e \cdot c^2} \cdot \frac{M}{m_e}} - 1\right). \tag{5}$$

After Pauling (1954) the displacement energy is related to the binding energy of the atomic bond and is about twice the binding energy. Figure 2 gives an empirical presentation of the displacement energy against reciprocal lattice constant (Corbett and Bourgoin, 1975). This is a purely phenomenological approach and can be helpful to gain a first order value of T_d.

In order to describe a differential cross-section, Mott (1929, 1932) treated the case of electrons and derived a comprehensive solution, however his expression is not very handy. McKinley and Feshbach (1948) developed an approximation, which can be handled very easily and which is given in the following form

$$\frac{d\sigma_d}{dT_2} = \frac{Z^2 \cdot e^4 \cdot (1-\beta^2)}{4 \cdot u^2 \cdot \beta^4 \cdot c^4} \cdot \frac{T_{2\max}}{T_2^2} \cdot \left(1 - \beta^2 \cdot \frac{T_2}{T_{2\max}} + \pi \cdot \alpha \cdot \beta \cdot Z \cdot \left(\left(\frac{T_2}{T_{2\max}}\right)^{1/2} - \frac{T_2}{T_{2\max}}\right)\right) \tag{6}$$

with the reduced mass unit $u = mM/(m+M)$, $\beta = v/c$ and $\alpha = 1/137$ the fine structure constant, Z the charge number of the target atom, e the elementary charge. The cross-section is then given by

$$\sigma_d(E_1) = \int_{E_d}^{T_{2\max}} P(T_2) \cdot \frac{d\sigma_d(E_1, T_2)}{dT_2} dT_2. \tag{7}$$

$P(E_2')$ is the probability that a lattice atom will be displaced and is generally taken as a step-function with

$$P(T_2)\begin{cases} = 0 & \text{for } T_2 < T_d \\ = 1 & \text{for } T_2 \geqslant T_d. \end{cases}$$

However, it is very unlikely that there is a very sharp energy threshold and each hit above this value results

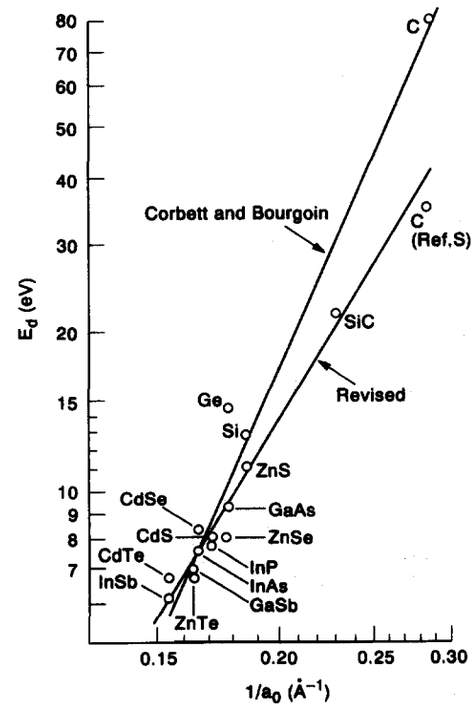

Fig. 2. T_d of various materials vs reciprocal lattice constant after Corbet and Bourgoin (1975) and revised by Barry *et al.* (1991).

Table 1. Threshold energies E_{th} in keV for different particles and semiconductor materials

			GaAs		SiC	
	Si	Ge	Ga	As	Si	C
T_d in eV	21	27.5	7–11		21.8	
E_{th} (electrons)	220	580	188–275	200–292	220	108
E_{th} (protons)	0.15	0.5	0.12–0.19	0.13–0.21	0.15	0.065

in a displacement event and below that value there occurs nothing at all. There are several influences that can smear out this probability step. Among others there are:

- Crystal orientation (anisotropy effect);
- Lattice vibrations (temperature);
- Isotopic mixture;
- Electron straggling (depth dependence);
- Impurities;
- Multiple defects.

However the displacement threshold T_d is an important quantity for modelling of the displacement damage or, speaking more specific, of the defect introduction rate. Figure 3 shows an example for ⟨100⟩ and ⟨111⟩ GaAs (Lehmann and Bräunig, 1993). It is quite obvious that a graded probability function fits the GaAs ⟨100⟩ data well, whereas the GaAs ⟨111⟩ data agree with the step-function, as shown in the inset.

As a consequence of several uncertainties in the modelling of defect introduction and generation of displacement damage, experimental data are needed. This will be introduced in the following part before we describe a different approach of theoretical modelling, the Non-Ionizing Energy Loss (NIEL).

2.3. *The concept of the damage factor*

By generating additional electrically active centers within the semiconductor material some properties of the material can be changed, which are directly accessible to the experiment. For instance, the minority carrier lifetime τ is defined as

$$\tau = \frac{1}{\sigma \cdot v_{th} \cdot N_t} \tag{8}$$

where σ is the capture cross-section, v_{th} the thermal velocity and N_t the concentration of electrically active centres in cm^{-3}. In a very simple way the addition of radiation induced defects $N_{t\,rad}$ can be described by

$$N_t + N_{t\,rad} = \frac{1}{\sigma \cdot v_{th}} \cdot \frac{1}{\tau_1} \tag{9}$$

where τ_1 is the post-radiation lifetime ($\tau_1 < \tau_0, \tau_0$ being the initial lifetime). This yields the relation

$$\Delta\left(\frac{1}{\tau}\right) = \frac{1}{\tau_1} - \frac{1}{\tau_0} = \sigma \cdot v_{th} \cdot N_{t\,rad}. \tag{10}$$

On the other hand the following holds

$$N_{t\,rad} = \sigma_d \cdot N_A \cdot \Phi \tag{11}$$

with σ_d the total displacement cross-section [see

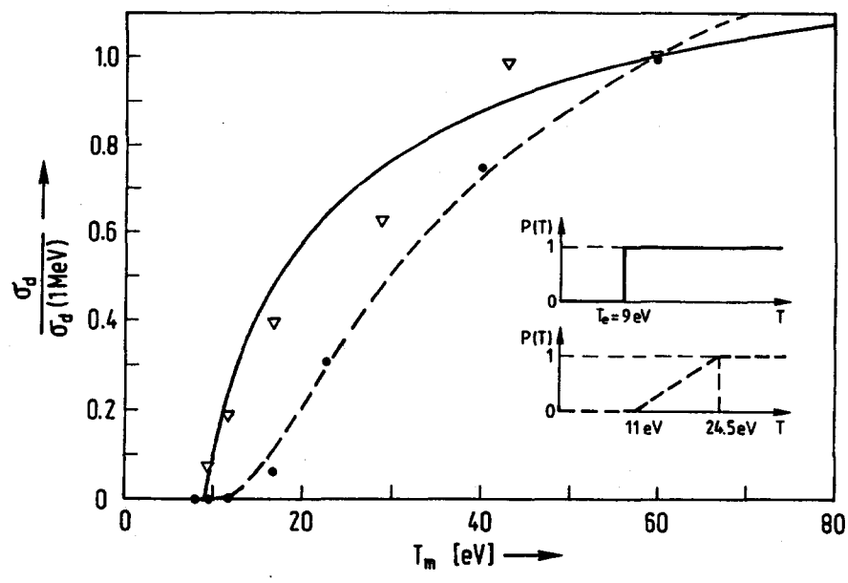

Fig. 3. Defect introduction rate vs energy for ⟨111⟩ (solid) and ⟨100⟩ (dashed) GaAs. The insert shows the different functions for the displacement probability (Lehmann and Bräunig, 1993).

Table 2. The damage factor k_τ in cm^2/s for 3 MeV-electrons, 20 MeV-protons and 1-MeV-neutrons for Si and various resistivities

	Substrate resistivity in Ω cm				
Injection level		Low (<1E−2)		High (>1)	
3-MeV-electrons	n-type				
	1	(0.6–3)E−7		≈5E−8	
	10	(2–10)E−8		≈1E−8	
	p-type				
	1	(1–4)E−8		(2–8)E−9	
	10	(0.5–2)E−8		(1–4)E−9	
	100	≈3E−9		≈6E−10	
Injection level		1E−3		1E−1	
20-MeV-protons	n-type				
	1	(2–10)E−5		(1–5)E−5	
	10	—		≈5E-6	
	p-type				
	1	(1–3)E−5		≈1E−6	
	10	—		≈5E−6	
Injection level		1E−5	1E−3	1E−1	1
1-MeV-neutrons	n-type				
	1	1E−5	5E−6	2E−6	1.5E−6
	10	6E−6	3E−6	1.5E−6	1E−6
	100	1E−5	2.5E−6	5E−7	3E−7
	p-type				
	1	8E−6	2E−6	5E−7	3E−7
	10	8E−6	2E−6	5E−7	3E−7
	100	2.5E−6	1.5E−6	5E−7	—

equation (7)], N_A being the number of lattice atomsper unit volume and Φ the particle fluence per unit area. Combining equations (10) and (11) yields

$$\Delta\left(\frac{1}{\tau}\right) = \underbrace{\sigma \cdot v_{th} \cdot \sigma_d \cdot N_A}_{k_\tau} \cdot \Phi = k_\tau \cdot \Phi. \tag{12}$$

k_τ is called the damage factor or damage coefficient and is commonly used as a very powerful tool to describe the behaviour of a semiconductor device after irradiation. It is at least required that k_τ is independent of the fluence and this is fulfilled for fluences not so high that the wave functions of the damage centres do overlap. Extensive experimental work is carried out in order to determine the damage factor of Si. Here especially for neutrons a bulk of knowledge exists, but the more abundant species in space, electrons and protons, are also present (van Lint *et al.* 1980, 1975; Bräunig, 1989). Table 2 gives the values of k_τ for a number of resistivities and injection levels (this quantity is the ratio of excess carriers to majority carriers) and electrons, protons and neutrons at a specified standard energy.

To cover the whole energy range, Fig. 4 gives the energy dependence of the damage factor for the individual radiation species, where the damage factor is normalized to that value at the standard energies.

The minority carrier lifetime represents the most sensitive semiconductor quantity, but in some cases the apparent change of doping (carrier removal) or the change of mobility are required. In a way similar to the approach for the lifetime damage factor the following definitions are established.

Carrier removal

$$n = n_0 - \left(\frac{\Delta n}{\Delta \Phi}\right) \cdot \Phi \tag{13}$$

and the change in carrier mobility

$$\frac{1}{\mu} = \frac{1}{\mu_0} + k_\mu \cdot \Phi \tag{14}$$

For 1 MeV-neutrons in Si the following values hold (Ziegler *et al.*, 1985): $(\Delta n/\Delta\Phi) = 6$ $(n \cdot s)^{-1}$ and $k_\mu = 3 \cdot 10^{-19}$ V·s/n. The use of the damage factor concept enables the application engineer to check quantitatively the irradiation induced degradation of a certain device parameter, which is a function of e.g. the minority carrier lifetime τ. This includes, for instance, the d.c.-current gain of a bipolar transistor or the spectral yield of a solar cell or other important properties of bipolar devices. From Table 2 it is obvious that p-type Si is more resistant against displacement damage than n-type material and that has some impact on hardening of solar cells (see also Crabb, 1994).

Let us assume as a simplified example a bipolar pnp-transistor and the common-emitter d.c.-current gain β according to the well-known WEBSTER-equation. Leaving only the irradiation sensitive parts and arranging for the change in reciprocal β we arrive

at

$$\Delta\left(\frac{1}{\beta}\right)=\frac{1}{\beta_{irr}}-\frac{1}{\beta}$$
$$=\underbrace{\frac{1}{2}\cdot\frac{w_B^2}{D_{pB}}\cdot\Delta\left(\frac{1}{\tau}\right)}_{(1)}$$
$$+\underbrace{\frac{N_{DB}\cdot w_B\cdot w_{EB}}{2\cdot D_{pB}\cdot n_i}\cdot\exp\left(\frac{-q\cdot V_{EB}}{2\cdot k\cdot T}\right)\cdot\Delta\left(\frac{1}{\tau}\right)}_{(2)}$$
$$\left(\underbrace{+\frac{N_{DB}\cdot w_B}{2\cdot D_{pB}\cdot n_i}\cdot\frac{A_s}{A_j}\cdot\exp\left(\frac{-q\cdot V_{EB}}{2\cdot k\cdot T}\right)\cdot\Delta(s).}_{(3)}\right) \tag{15}$$

Here β_{irr} is the current gain after irradiation, w_B the base width and w_{EB} the depth of the emitter–base space charge region, N_{DB} the doping concentration of the base region, D_{pB} the diffusion coefficient of holes within the base ($=L_{pB}^2/\tau$), n_i the intrinsic carrier concentration, V_{EB} the emitter–base voltage and kT/q the thermal voltage. The term labelled (1) is the portion governed by the base transport factor, (2) repesents the volume space-charge recombination within the emitter–base junction and term (3) is the surface recombination portion, which will be omitted here and will be of concern in the Section 4 of this paper. $\Delta(1/\tau)$ was introduced before and can be replaced by $k_\tau\cdot\Phi$ according to the damage factor concept. Therefore it is possible to describe the change in the d.c.-current gain as a function of fluence and emitter current ($\sim\exp(-qV_{EB}/kT)$). Regarding the relative importance of terms (1) and (2) term (2) is commonly negligible at VEB-voltages > 500 mV compared to term (1) and equation (15) reduces to

$$\Delta\left(\frac{1}{\beta}\right)=\underbrace{\frac{1}{2}\cdot\frac{w_B^2}{D_{pB}}}_{t_{tr}}\cdot k_\tau\cdot\Phi \tag{16}$$

where t_{tr} is just the transit time of holes across the base region. This quantity is related to the cut-off frequency by $f_{tr}=1/(2\cdot\pi\cdot t_{tr})$. As a first result, equation (16) suggests, that high-frequency transistors are much more radiation resistant than their low-frequency counterparts and this is true as a rule of thumb: reduce base width to get radiation hardness. There is a clear order from power- and small-signal transistors at the weak end and high-speed digital devices at the rad-hard regime. In addition most experimental results show a linear relationship between change of reciprocal gain and fluence as would be expected from equation (16) (Fig. 5) (Bäuerlein, 1968). A second rule of thumb is, that a transistor should operate in the high collector current range, where the $\beta(I_C)$ characteristic is almost flat.

A great variety of electrical parameters of semiconductor devices depends on the minority carrier lifetime and all these quantities are affected in a analogous way. The efficiency of solar cells, for example, depends on the diffusion length and any degradation results in loss of yield, most pronounced in the infra-red regime. In other cases, where the leakage current is of importance, an increase is a direct result of displacement damage. At higher fluences the apparent reduction of doping concentration (carrier removal) results in increased bulk resistances, which is specifically important for power or majority carrier devices. The reduction of mobility, at high fluencies, is most pronounced at low temperatures in particular, when scattering at defects dominates. In order to get a feeling of the vulnerability of current devices most of modern devices withstand a neutron fluence of $10^{14}\,cm^{-2}$, but $10^{15}\,cm^{-2}$ is a critical fluence for most of the digital ICs. Bipolar

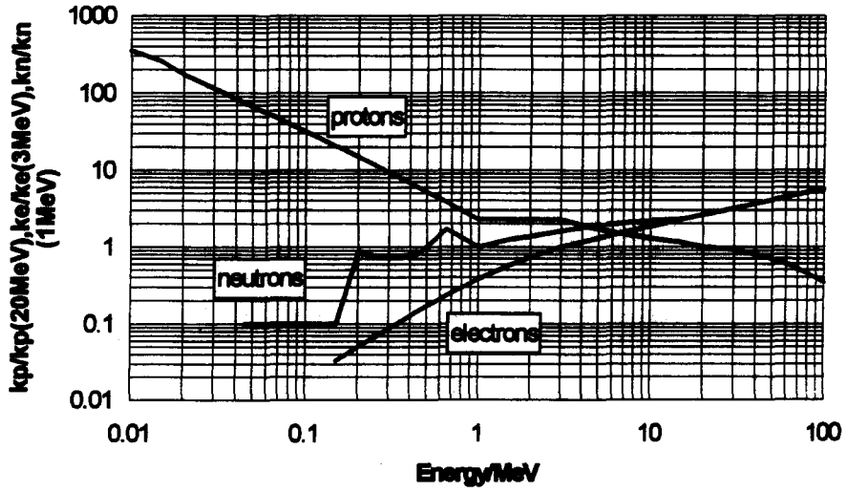

Fig. 4. The ratio of damage factors for electrons (3 MeV), protons (20 MeV), neutrons (1 MeV) according to $k_\tau(E)/k_\tau$ (at standard energy).

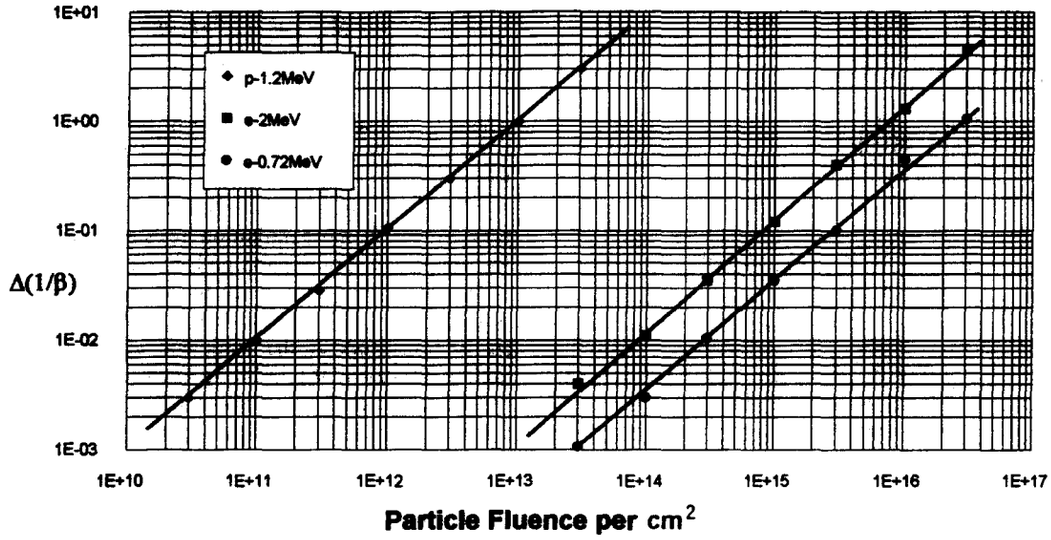

Fig. 5. Change of reciprocal gain of an npn-Mesa-transistor BUY 14 at $I_C = 2$ A for protons and electrons at different energies (Bauerlein, 1968).

circuits are generally more sensitive. Here the radiation species are neutrons, but the range of fluence can easily be translated to other radiation species by using Table 2 and Fig. 4.

2.4. Non-ionizing energy loss (NIEL)

The need for displacement damage data of materials different from Si and especially for high energy protons, which are of prime concern in the space environment caused a renewed effort for a theoretical clarification. As pointed out in Section 2.1 the electron interaction with the target material is considered as purely elastic scattering. In the case of high energetic protons inelastic scattering can dominate. Here the rate of damage introduction is given by the non ionising contribution to damage, which is called NIEL (Non Ionizing Energy Loss). It is defined by (Summers, 1992)

$$\mathrm{NIEL} = \frac{N}{A} \cdot (\sigma_e \cdot T_e \cdot \sigma_i \cdot T_i). \tag{17}$$

The units of NIEL is eV·cm²/g, N/A is the atomic density (A = Avogadro number and N = gram atomic weight), σ the total cross-sections and T the average recoil energy. The index e stands for elastic and i for inelastic interaction. A more accurate estimation is based on the differential cross-section instead of the total cross-section and is given by

$$\mathrm{NIEL} = \frac{N}{A} \cdot \int L[T(\Theta)] \cdot T(\Theta) \cdot \frac{\mathrm{d}\sigma}{\mathrm{d}T} \cdot \mathrm{d}T. \tag{18}$$

The lower limit of the integral is given by the

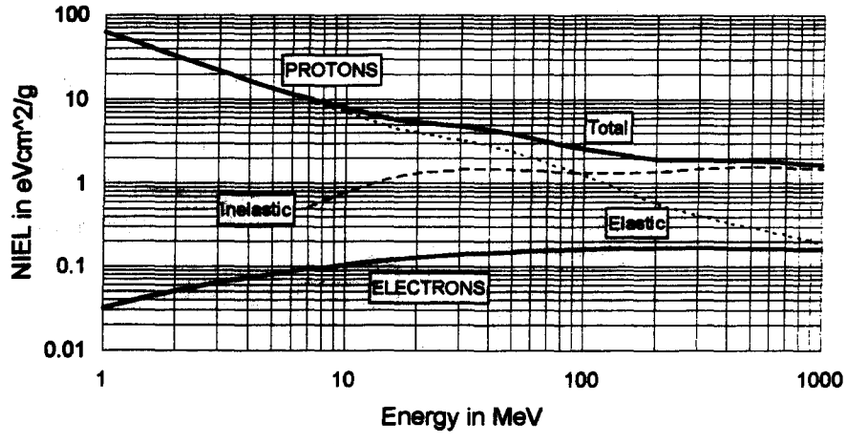

Fig. 6. NIEL calculations for electrons and protons versus incident energy in Si (Summer, 1992). Note that for protons the energy loss due to inelastic scattering dominates that of elastic scattering above 100 MeV.

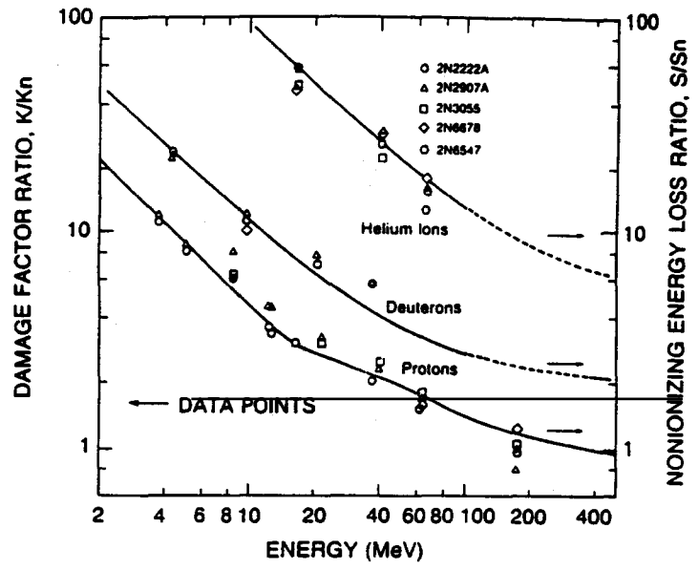

Fig. 7. Experimental damage factor and NIEL ratios vs energy for protons, deuterons and αs.

displacement threshold energy [see equation (5)] and the upper limit is given by equations (2) or (3). $d\sigma/dT$ is the differential cross-section for a recoil in direction Θ and $L[T(\Theta)]$ is the fraction of recoil energy, which goes into displacement. This kind of calculation can be made with Monte-Carlo calculations such as TRIM (Ziegler *et al.*, 1985). Without going into the underlying physical models and assumptions two results are presented which show the effectiveness of the NIEL concept. Figure 6 shows the NIEL of electrons and protons against energy (Summers, 1992) and Fig. 7 illustrates the similarity of calculated NIEL and experimentally obtained data (Summers *et al.*, 1987).

2.5. Microdosimetry effects

So far the prediction tools were based on a macroscopic scale in terms of semiconductor material or device parameters. With shrinking device dimensions microscopic effects of damage behaviour gain importance in analogy to the LET concept for Single Event Phenomena. For instance the minority carriers lifetime τ, as given by equation (8), is inversely proportional to the defect concentration N_t. With v_{th} in the order of 10^7 cm/s and σ in the order of 10^{-14} cm^2 and a currently obtainable lifetime τ in the order of 100 μs the number of defect centres is 10^{11} cm^{-3}. The size of a pixel cell of a CCD or CID can reach 2×4 μm. Assuming an active depletion depth of 10 μm the active volume sums up to 80 $(\mu m)^3$ or $8 \cdot 10^{-11}$ cm^3. Thus, only 8 defect centres are responsible for the dark current via the lifetime and adding only the same number by displacement damage would double the dark current. This illustrates the need for leaving the large number average mechanisms and to enter the statistical behaviour for these small devices.

Srour *et al.* (1986) showed for the first time that single protons can produce generation centres in a CCD, which are acting as additional current sources to the dark current and these centres are created on a probabilistic basis. An interesting feature of these experiments are, besides the impact on the functionality of this particular device, the expectation of gaining increased information about the underlying physics of interaction. Of primary concern is the partitioning of elastic and inelastic nuclear scattering especially for energetic protons. Dale *et al.* (1989) performed an extensive study of the fluctuations in the dark current of a 61504 pixel CID after neutron and proton bombardment. Some of their results are shown in Fig. 8. Due to the probabilistic nature of the defect creation the dark current changes of the individual cells are distributed and skewed becoming more Gaussian, when the number of events increases. This can be described by the total relative variance V_T

$$V_T = \left(\frac{\sigma}{\mu}\right)^2 \tag{19}$$

where σ is the standard deviation and μ the mean value of the distribution. V_T is given by (Kellerer, 1985)

$$V_T = \frac{V_1 + 1}{N}. \tag{20}$$

Here N is the number of events and V_1 is the relative variance of a single event. According to equation (11) the number of displacement events is $N = \sigma_d \cdot N_A \cdot V \cdot \Phi$. As seen from Fig. 8 the number of events at a specific fluence differs largely for 12 MeV protons and fission neutrons. This fluctuation poses a fundamental limit of small sized devices and it seems that this limit is already reached in currently used ICs. The NIEL approach seems to be an adequate means for the prediction of these effects.

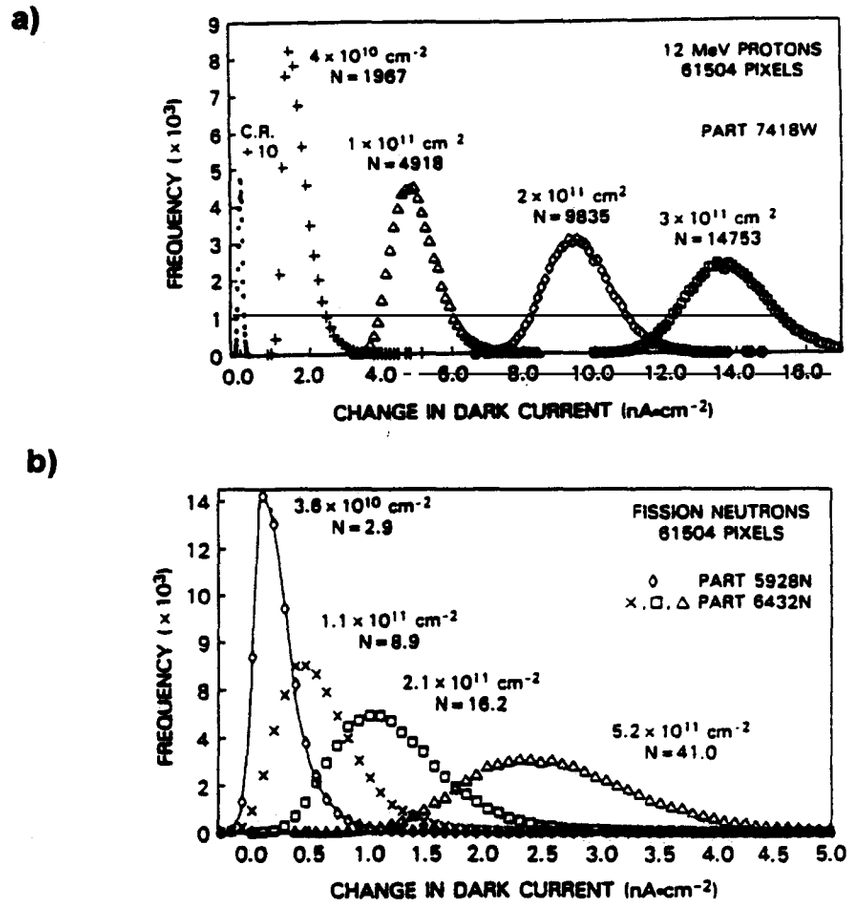

Fig. 8. Fluctuation in dark current change of CID pixel cells as a function of fluence for protons (a) and fission neutrons (b).

2.6. Test considerations

The only parts in a space environment affected by displacement damage are solar cells and low-frequency bipolar transistors. The particles under concern for this type of damage are protons and electrons and both are heavily ionizing as well. Testing is accomplished by a step-stress approach and the radiation sources, mostly used, are van de Graaff accelerators and high energy protons from cyclotrons and linear accelerators. When neutrons are used they come from nuclear reactors and neutron generators. In the case of a spectral distribution of the radiation species it is advisable to calculate the equivalent fluence at the standard energies as mentioned in Section 2.3 according to Fig. 4 and Table 2 by using the following equation (21)

$$k_{\mathrm{stand}} \cdot \Phi(E_{\mathrm{stand}}) = \sum_i k(E_i) \cdot \Phi(E_i). \qquad (21)$$

Here, all the individual spectral contributions are summed up in their effectiveness in producing displacement defects.

3. TOTAL IONIZING DOSE EFFECTS ON SEMICONDUCTOR DEVICES

3.1. Introduction

Total ionizing dose effects (TID), also often called total dose effects on electronic devices and circuits have been studied for more than 25 years, but up to now the complex interactions are not fully understood. Different models are used to predict the behaviour of the prompt and delayed radiation response of electronic devices. In this section only a brief review of the basic effects will be discussed. The aim of this review is to introduce the problems involved in the prediction of the radiation hardness of electronic devices used for space applications.

The TID has the strongest impact on MOS devices and circuits which use passivation layers in the active area of the transistors like advanced bipolar technology. Therefore the following description is limited to these technologies.

3.2. Basic mechanisms

Some preliminary explanations about the interaction of ionizing particles and electromagnetic

quanta with the insulating layers of the MOS technology are necessary to understand the degradation mechanisms of semiconductor devices. The first effect is the transfer of energy to the matter quantified by the absorbed dose and the second step is the generation of electron–hole pairs and their impact on the insulating material.

3.2.1. Dosimetry. High energy particles, electrons, protons, electromagnetic quanta interact with matter in different ways but they always lose energy in the irradiated volume. The *absorbed dose*, often called *dose* or *total dose*, D, gives the mean energy absorbed per unit mass of irradiated material at the point of interest (ICRU, 1980; ASTM, 1985)

$$D = \frac{dE}{dm} = \frac{1}{\rho} \cdot \frac{dE}{dV} \tag{22}$$

E: energy (J); m: mass (kg); ρ: density (kg/dm^3); V: volume (dm^3). The SI unit of dose is the gray (Gy):

$$1\ \text{Gy} = 1\ \text{J/kg}. \tag{23}$$

Due to the different atomic properties of the target material, the absorbed dose depends on the material of interest and therefore the specific material should always be referenced in parentheses of the unit rad or Gy [e.g. rad(Si), Gy(Si)]. The use of the gray has been strongly advocated by the various standard organizations but the rad is still used by many experimenters and in many applications.

1 Gy = 100 rad with the definition of:

$$1\ \text{rad} = 100\ \text{erg/g}. \tag{24}$$

The material of interest to the MOS technology is silicon (Si) and silicon dioxide (SiO_2). The stopping power in Si and SiO_2 is nearly the same for photon energies above 1 keV (Hamm, 1986). Therefore the specified material for MOS devices is silicon [rad (Si) or Gy (Si)].

The *absorbed dose rate* (also often called *dose rate*) D' is the time rate of the absorbed dose (ASTM, 1985)

$$D' = \frac{dD}{dt}. \tag{25}$$

Ionizing radiation can be performed by X-rays, γ-rays and electrons. The absorbed dose depends on the photon or particle energy and the density of the absorbing material. Photons have no zero rest mass and are electrically neutral. They interact with target atoms by the photoelectric effect, Compton scattering and pair production. The three photon interactions are a function of the target mass and photon energy. In the case of silicon, the photoelectric effect dominates at energies $E_{Ph} < 50$ keV and pair production dominates at energies $E_{Ph} > 20$ MeV. In the intermediate energy range, Compton scattering dominates (Evans, 1955). It should be noted that there is no physical process which transfers energy from photons directly to matter. Energy deposition by photons is therefore always a two-step process (Hubbell, 1969):

(i) a photon transfers energy to an electron;
(ii) the electron deposits a part or all of its kinetic energy on matter.

This leads to the important concept of photon and electron dosimetry, the charge particle equilibrium (CPE) (Hubbell, 1969; IEC 544-1). CPE is reached when the total energy carried out of the mass element dm by electrons is equal to the energy carried into it by electrons (Hubbell, 1969; IEC 544-1). This requires a minimum thickness of material which is called the equilibrium thickness. The equilibrium thickness depends on the density of the target material and the energy spectrum of the radiation. An accurate dosimetry with commonly used thermoluminescence dosimeter (TLD) can only be reached under CPE. A general method for determining equilibrium capsule thickness is given in ASTM Standard E665 and detailed procedures for the use of TLD in radiation hardness testing are given in ASTM Standard E668. A guideline, how to transfer the absorbed dose from one material to another is provided in ASTM Standard E666 and IEC544-1.

In layered structures like CMOS devices, the CPE especially for low energy photons in particular cannot be reached. This leads to the phenomenon of interface absorbed dose enhancement (also called interface dose enhancement, or dose enhancement) (Fleetwood *et al.*, 1988; Burke and Garth, 1976; Chadsy, 1978; Garth *et al.*, 1975; Wall and Burke, 1970; Garth, 1986). Dose enhancement effects as well as differences in electron–hole recombination as a function of the electric field (Fleetwood *et al.*, 1988; Brown, 1980; Dozier and Brown, 1980, 1981; Brown and Dozier, 1981a) must be taken into account when results of low energy X-rays (some keV) are compared with Co-60 irradiation of MOS devices. Depending on the type structure of the layers their difference in the prompt radiation response can be up to a factor of 4 (Dozier and Brown, 1983). Nevertheless, the difference in the relative response of MOS devices due to Co-60 γ and low energy X-rays (10 keV) irradiation cannot only be explained in terms of electron–hole recombination and dose enhancement effects (Fleetwood and Winokur, 1988).

3.3. Generation of oxide charges and interface states in SiO_2

3.3.1. Charge generation and recombination. For the practical solution of charge generation it can be supposed that the absorbed energy in the material is totally used to create electron–hole (e–h) pairs. The energy needed to create one e–h pair in SiO_2 is $E_{e\text{-}h} = 18\ \text{eV} \pm 1\ \text{eV}$ (Ausmann and McLean, 1975; Curtis *et al.*, 1974). More accurate sets of measurements and analysis have shown a value of $E_{e\text{-}h} = 17\ \text{eV} \pm 1\ \text{eV}$ (Beneto and Boesch, 1986), but the value of $E_{e\text{-}h} = 18\ \text{eV}$ is still used. The typical ionizing energies and e–h density generation factors

Table 3. Electron–hole (e–h) pair generation energies and pair density generation factors of different materials (Srour, 1983)

Material	$E_{e\text{-}h}$ [eV]	g_0 [e–h/(Gy · cm^3)]
Silicon Si	3.6	$4.0 \cdot 10^{15}$
Silicon dioxide SiO_2	18	$8.2 \cdot 10^{14}$
Galium arsenide GaAs	~4.8	$\sim 7 \cdot 10^{15}$
Germanium Ge	2.8	$1.2 \cdot 10^{16}$

g_0 of some semiconductor materials are summarized in Table 3.

Immediately after the first phase of e–h pair generation there is a stage of recombination. Some of the electrons and holes generated initially recombine in less than picoseconds. Only a fraction of the primary generated e–h pairs remains in the oxide. The recombination rate is dependent on the particle energy and type and the oxide field. Two basic models are used to describe the ionization and recombination process of e–h pairs in insulators:

(i) the *columnar model*, where the e–h pairs are very close together (Jaffe, 1914; Bragg and Kleeman, 1906; Langevin, 1903 a,b; Oldham, 1982, 1985; Oldham and McGarrity, 1983) and
(ii) the *geminate model*, where the charge density N along the ionizing track is smaller (Onsager, 1934, 1938; Ausman, 1986).

These models are determined by two parameters:

(i) the *thermalization distance* r_t which characterizes the initial separation between the hole and its corresponding electron after reaching their thermal energy and
(ii) the *mean separation distance* λ between the e–h pairs.

In SiO_2 the thermalization distance is in the order of 5–10 nm. The separation distance is inversely proportional to the charge generation per cm. The generation of e–h pairs is proportional to the electronic stopping power dE/dx.

$$N = \frac{\rho}{E_{e\text{-}h}} \cdot \frac{dE}{dx} \tag{26}$$

$$\lambda = \frac{1}{N} \tag{27}$$

N: charge density (cm^{-1}); ρ: density (g/cm^3); dE/dx: electronic stopping power (eV/g/cm^2).

For electrons, X-rays and Co-60 irradiation, the geminate model describes the experimental results sufficiently. Only for low energy radiation with a stopping power greater than 10 MeV/g/cm^2 do the effects of the columnar and geminate model overlap and a modified model must be used (Bragg and Kleeman, 1906; McLean *et al.*, 1989). An intermediary model has been developed by Brown and Dozier (1981a,b). This model is valid only for sufficiently large electric fields ($E_{ox} > 0.5$ MV/cm), otherwise the diffusion effects of the carrier cannot be neglected.

In summary, the charge generation and recombination of holes in silicon dioxide is a very complex phenomenon depending on the radiation type (particle or quanta), its energy and the oxide field. Especially for low energy X-rays the effects of multilayer structures with different densities must be taken into account. In practice X-ray and Co-60 sources are used for the irradiation testing of electronic devices. Dozer *et al.* (1987) have summarized different results of radiation experiments to find an empirical solution for the fraction of holes which escape recombination after Co-60 and 10 keV X-ray irradiations as a function of the applied oxide field. The following empirical formulas for the fraction hole yield f_h have been found:

$$f_h(E_{ox}) = \left(\frac{0.5}{E_{ox}} + 1\right)^{-0.7} \quad \text{Co-60} \tag{28}$$

$$f_h(E_{ox}) = \left(\frac{1.35}{E_{ox}} + 1\right)^{-0.9} \quad \text{X-ray} \tag{29}$$

E_{ox}: oxide field (MV/cm).

3.3.2. Transport of charges in the oxide. The phenomena of charge generation and recombination are essentially completed after some picoseconds. After this time, the excess electrons and holes are free to undergo transport in the SiO_2 layer depending on the electric field. Electrons have a high mobility of $\mu_e = 20$ cm^2/V s at 300 K and an increasing mobility at lower temperatures ($\mu_e = 40$ cm^2/V s at 114 K) (Hughes, 1973, 1975a, 1978; Othmer and Srour, 1980). The maximum velocity is about $1 \cdot 10^7$ cm/s (Srour *et al.*, 1974; Ferry, 1979). After some picoseconds the electrons are swept out of the oxide ($d_{ox} < 100$ nm) and are collected at the positive electrode. The mobility of the holes is $1.6 \cdot 10^{-5}$ cm^2/V s at 300 K and is strongly temperature dependent. The thermal activation energy is determined by 0.16 eV (Hughes, 1975b, 1977; Hughes *et al.*, 1975). The mobility μ_h is a zero field mobility and does not explain the time dispersive transport of the holes in the SiO_2 after short pulse irradiation (McLean *et al.*, 1978; Boesch *et al.*, 1978, 1985). The hole transport in SiO_2 can be described by the continuous time random walk (CTRW) model. Based on the work of Montroll and Weis (1965) together with Pfister and Scher's (Scher and Montroll, 1975; Scher and Lax, 1973; Fister and Scher, 1978) stochastic transport model, Boesch *et al.* (1975, 1978) and McLean (McLean *et al.*, 1975, 1976; McLean and Ausmann, 1977) developed this model for the hole transport in silicon dioxide via polaron hopping between localized sites. A second model from Curtis and Srour (1977) describes the transport by multitrapping of holes in single level states. The most appropriated CTRW model uses a probability function $\psi(t) \sim t^{-(1+\alpha)}$ for the random hopping process of the holes. The typical values of the disorder parameter α in amorphous silicon dioxide are in the range of $\alpha = 0.15$–0.35 (Boesch *et al.*, 1975; McLean *et al.*, 1975).

The recovery behaviour of the flatband voltage shift after short pulse electron irradiation as a function of the oxide field and temperature can be

explained by the characteristic time t_s. In practice, t_s may be taken as the time that half recovery $t_{1/2}$ of the flatband voltage shift occurs. For temperature $T > 140$ K the characteristic time t_s is given by (McLean and Oldham, 1987; McLean *et al.*, 1989)

$$t_s = t_s^0 \cdot \left(\frac{d_{ox}}{a}\right)^{1/\alpha} \cdot \exp\left(\frac{\Delta(E_{ox})}{kT}\right) \tag{30}$$

t_s^0: constant (s); a: average hopping distance in the field direction (nm); α: disorder parameter; $\Delta(E_{ox})$: field dependent activation energy (eV); d_{ox}: oxide thickness (nm).

The field dependence of the activation energy is small and fitted by the following function:

$$\Delta(E_{ox}) = \Delta_0 - b \cdot E_{ox} \tag{31}$$

Δ_0: low field limit of $\Delta(E_{ox})$ (eV); b: fitting parameter.

Typical values for hardened SiO_2 are: $\alpha = 0.25$, a = 0.1 nm, $\Delta_0 = 0.65$ eV, $b = 0.05$ eV/MV/cm and $t_s^0 = 10^{-22}$ s.

It should be noted that the characteristic time t_s is superlinear thickness dependent:

$$t_s \sim d_{ox}^{1/\alpha}; \quad \text{with } \alpha = 0.25 \quad t_s \sim d_{ox}^4.$$

The CTRW model is a well accepted model for the description of the dispersive transport of holes in SiO_2.

3.3.3. Hole and electron trapping. Under the influence of the electrical field in the oxide the holes move to the SiO_2/Si or SiO_2/gate interface. At these interfaces a fraction of them are trapped in deep hole traps. The remaining holes recombine with the electrons of the gate or from the substrate contact. Trapped oxide charges N_{ot} at the SiO_2/Si interface have the strongest effect on the threshold voltage shift of MOS transistors. The distance of the charge centroid of the N_{ot} from the SiO_2/Si interface is in the range of 3–13 nm (Wood and Williams, 1976; Manchanda *et al.*, 1981; Freeman and Holmes-Siedle, 1978; Viswanathan and Maserjian, 1976; Hughes and Powel, 1976; Grunthaner *et al.*, 1977a,b; Chang and Lyon, 1986; Di Maria *et al.*, 1975; Di Maria, 1976; Powel and Berlund, 1971; Hu, 1980), with a typical value of 4–5 nm (Lipkin *et al.*, 1990). The range of the hole trap density is 10^{12} to 10^{13} cm^{-2} (Lipkin *et al.*, 1990; Young *et al.*, 1979; Aiken and Young, 1977). The conditions under which MOS devices are produced have a strong impact on the initial hole trap density $N_{t\infty}$. The hole traps are characterized by a high capture cross section σ_h in the order of 10^{-14} to 10^{-13} cm^{-2} (Lipkin *et al.*, 1990a, Aikin and Young, 1977; Schwerin *et al.*, 1990; Boesch *et al.*, 1986; Ning, 1976). This σ_h value is typical for Coulomb attractive centers. Their field dependence should be proportional to $E^{-3/2}$. Ning (1976) has found a field dependence proportional to $E^{-3/2}$ for oxide field $E_{ox} < 0.7$ MV/cm and E^{-3} for higher fields. Other experimental results have shown a weaker proportionality (Schwerin *et al.*, 1990) or values of $E^{-0.6}$ and $E^{-0.4}$ (Tzou *et al.*, 1983). A complete model of capture cross sections must include the recombination of electrons with trapped holes (Ning, 1976; Clement, 1978).

There are also electron traps in the oxide, but at 10^{-17} to 10^{-18} cm^2 the electron capture cross section σ_e is three orders of magnitude lower than the hole capture cross section (Di Maria and Stasiak, 1989). The charge centroid of the electron trap density is about 9 nm from the SiO_2/Si interface (Young *et al.*, 1979). In the case of ionizing radiation the capture of electrons in electron traps can be neglected.

3.3.4. Microscopic nature of hole traps and interface states. From electrical measurement it is not possible to provide information on the physical nature of the hole traps. Only physical analysis techniques such as X-ray photoelectron spectroscopy (XPS) (Gunthaner *et al.*, 1979a,b), electron spin resonance (ESR) (Sigel *et al.*, 1974; Lenahan and Dressendorfer, 1982; 1983a, 1984a,b; Kim and Lenahan, 1988) or optical spectroscopy throw some light on the inside of the defect structure of the SiO_2. Most of the basic work has been performed on quartz and fused silica in addition to thermally grown oxide used for MOS technology. In this section only a brief summary of results and models can be examined. More details can be found in McLean *et al.* (1989) and Griscom and Friebele (1982).

In general a distinction can be made between *intrinsic* (structural) and *extrinsic* (impurity related) defects.

Intrinsic defects: In the first region (1–4 nm) of the thermally grown oxide a substantial density of strained Si–O–Si bonds were found. The normal 144° bond angle of the bulk SiO_2 network is reduced to 120° and the density of these strained bond is lower in radiation hard oxides than in radiation soft oxides (Grunthaner and Maserjian, 1978). These strained bonds are broken by a hole or by the radiation itself generating a trivalent silicon which is positively charged. The mobile nonbridging oxygen defect migrates under the strain gradient to the SiO_2/Si interface (Grunthaner *et al.*, 1982). This generation process leads to the bond-strain gradient (BSG) model (Grunthaner *et al.*, 1982).

It has already been suggested by Revesz (1971) that hole trapping in SiO_2 is an intrinsic property of the Si—O bond. The formation of nonbridging oxygen and trivalent silicon reacts as a hole trap. Another defect in the SiO_2 is the oxygen vacancy Si...Si, has been identified by ESR measurement as the E' center (Sigel *et al.*, 1974). The 1:1 correlation between the surface density of E' centers and the number of trapped oxide charges N_{ot} leads to the conclusion that the E' center is the precursor of the hole trap (Lenahan and Dressendorfer, 1983) (Fig. 10).

Extrinsic defects: The potential role of the ubiquitous water related hydrogen and hydroxyl ion impurities tying up dangling bonds during

processing has been emphasized by Revesz (1971, 1980a,b, 1981) and Balk (1965). For some years the role of the hydrogen and the hydrogen related defects becomes again the important question in understanding the long term stability of SiO_2. Two basic types of defects are the Si—OH and Si—H configurations. The Si—OH is an acceptor and the Si—H is a donator type defect, and the reaction with electrons and holes is as follows (Revesz, 1971) (see Fig. 10):

$$\text{Si—OH} + \text{e} \Rightarrow \text{Si—O}^- + \text{H}^0 \tag{32}$$

$$\text{Si—H} + \text{h} \Rightarrow \text{Si}^+ + \text{H}^0. \tag{33}$$

The trivalent silicon in the bulk of the SiO_2 bonded to three oxygen atoms is correlated to the E' center. Trivalent silicon at the SiO_2/Si interface back bonded to the silicon atoms of the substrate, is identified as a P_b-center and related to the interface state N_{it} (Poindexter and Caplan, 1981, 1983; Lenahan *et al.*, 1981; Lenahan and Dressendorfer, 1983b; Mukawa and Lenahan, 1984, 1985, 1986; Warren and Lenahan, 1986). By contrast to the E' center, the electrical state of the P_b-center is formed by the fermi level of the silicon. It should be noted that the same defect type is related to the positive trapped charge N_{ot} or to the interface state N_{it} only by the distance to the SiO_2/Si interface (Svensson, 1978) (see Fig. 10). Depending on the distance of the defects to the interface, the tunneling process of electrons into a trap and out of a trap is controlled. The distinctiveness of slow states and charging and discharging of traps can be understood in this physical picture.

The energy distribution of the interface state density $D_{it}(\varphi_s)$ can be correlated to the distance and type of the surrounding atoms of the trivalent silicon at the interface (Sakurai and Sugano, 1981).

3.3.5. Hole trapping factor. After the basic mechanisms of generation of electron–hole pairs and trapping of positive charges have been examined, the buildup of the oxide charge density N_{ot} as a function of the accumulated dose, oxide field and trap density can be summarized by a simplified model. Assuming that the oxide contains only one type of hole trap $N_{t\infty}$ with a capture cross section of σ_h, the trapping rate may be described by a first order kinetic equation:

$$\frac{\mathrm{d}\Delta N_{ot}}{\mathrm{d}t} = (N_{t\infty} - \Delta N_{ot}) \cdot I_{inj} \cdot \frac{\sigma_h}{q} \tag{34}$$

$$I_{inj} = q \cdot g_0 \cdot f_h(E_{ox}) \cdot d_{ox} \cdot D' \tag{35}$$

I_{inj}: generated current by the ionizing irradiation in the SiO_2 (A/cm^2); $N_{t\infty}$: initial defect density (cm^{-2}); g_0: e–h density generation factor (Table 3) [e–h/(Gy·cm^3)]; $f_h(E_{ox})$: fraction hole yield factor [of equations (28), (29)]; d_{ox}: oxide thickness (cm); D': dose rate (Gy/s); σ_h: capture cross section (cm^2); q: elementary charge (As).

Providing that ionizing irradiation does not generate new hole traps in the oxide [which was found to be true up to a maximum dose of 10^5 Gy(Si) (Lipkin *et al.*, 1990)] and the annealing of N_{ot} during the exposure time can be neglected, the following result is found:

$$\Delta N_{ot}(t) = N_{t\infty}\left(1 - \exp\left(-Q_{inj} \cdot \frac{\sigma_h}{q}\right)\right) \tag{36}$$

with

$$Q_{inj} = \int I_{inj} \cdot \mathrm{d}t. \tag{37}$$

Radiation hardness of different technologies or devices can be expressed by the hole trapping factor A introduced by Freeman and Holmes-Siedle (1978). Using the slope of the function at the time $t = 0$, the hole trapping factor can be defined as the ratio of the trapped charge density ΔQ_{ot} to the density of injected charges ΔQ_{inj}. The trapping factor is then the product of the capture cross section and the initial trap density:

$$\left|\frac{\mathrm{d}\Delta N_{ot}}{\mathrm{d}t}\right|_{t=0} = q \cdot g_0 \cdot f_h(E_{ox}) \cdot d_{ox} \cdot D' \cdot \frac{\sigma_h}{q} \cdot N_{t\infty} \tag{38}$$

$$A = \frac{\Delta Q_{ot}}{\Delta Q_{inj}} = \sigma_h \cdot N_{t\infty} \tag{39}$$

with

$$\Delta Q_{ot} = q \cdot \Delta N_{ot}. \tag{40}$$

Multiple capture cross sections and trap types have been found (Tzou *et al.*, 1983), but in practice this formula is sufficient to characterize the hole trapping behaviour of a MOS technology.

3.3.6. Annealing of trapped charges. Most of the trapped holes anneal with time. Two models are used for the description of the logarithmic time dependence of the annealing of N_{ot} after irradiation. The thermal emission model assumes the annealing of N_{ot} by thermal emission of holes from the traps in the oxide to the valence band. The annealing behaviour of N_{ot} as a function of the temperature and oxide field has been examined in great detail (Schwank *et al.*, 1984; Lelis *et al.*, 1989; Simons and Huges, 1971, 1972). McLean's tunnel model (McLean, 1976) assumes that the positive charges recombine with electrons tunneling from the substrate into the SiO_2. McWhorter *et al.* (1982) have derived a new model for predicting hole annealing by combining the tunnel and thermal model shown in Fig. 9. The tunnel front $X_m(t)$ moves into the SiO_2 with a velocity of about 0.2 mm per decade. The potential barrier high β is a function of the oxide field and the temperature (Lakshmanna and Vengurlekar, 1988). In general, the tunnel and thermal emission model are consistent with many experimental data (Derbenwick and Sander, 1977; Winokur and Boesch, 1981; Habing and Shafer, 1973; Brucker, 1981).

A good description of the annealing behaviour of N_{ot} as a function of temperature magnitude and direction of the oxide field is important for character-

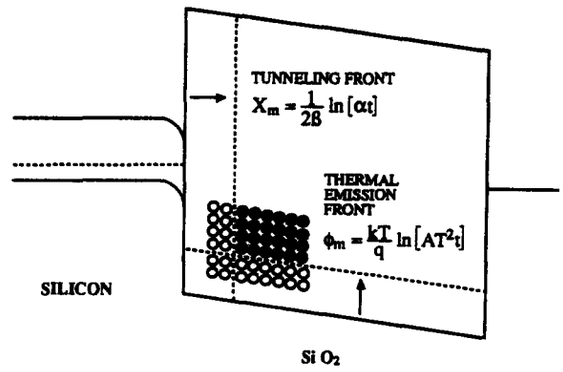

Fig. 9. Band diagram illustrating the two independent tunneling $X_m(t)$ and thermal emission $\phi_m(t)$ charge loss fronts (McWhorter *et al.*, 1990) with the parameters: β is the tunnel barrier height, α is attempt to the escape frequency, T the absolute temperature, q is the elementary charge, k is Boltzmann's constant and A depends on the capture cross section of the trap and other physical parameters.

izing of dose rate effects and the long term stability of irradiated MOS devices.

3.3.7. Generation of interface states. In addition to hole trapping in silicon dioxide, there is a buildup of interface states N_{it}. The prompt and delayed generation process is more complicated than the buildup of oxide charges. Many models have been proposed to explain the nature and generation process of these defects. In the two step model proposed by Lai (Lai, 1983), holes break strained Si—O—Si bonds at the SiO_2/Si interface and in the second step the N_{it} are formed by electron capture in these hole traps.

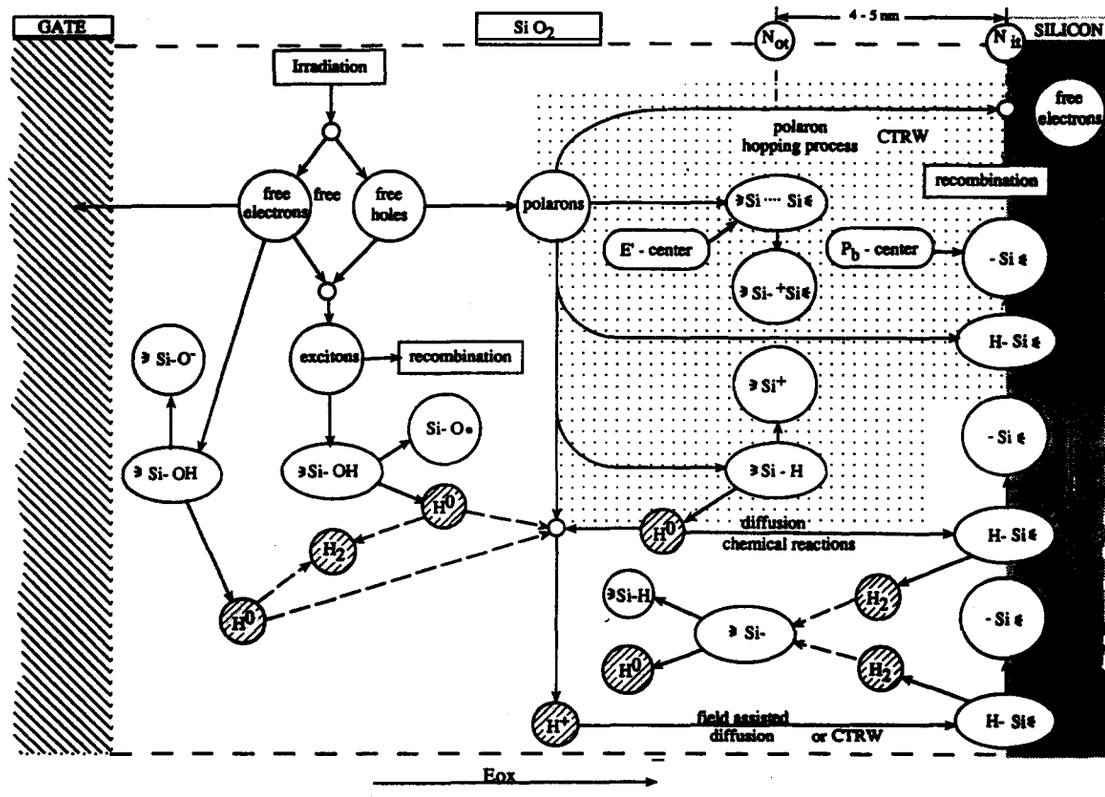

Fig. 10. Visualization of interactions of ionizing radiation with the SiO_2 and its interfaces in MOS structures. The ellipses represent the defects in the SiO_2 and the circles contain the reaction product. Reactions of the holes with the SiO_2 are marked by the dotted area. Released hydrogen is marked by shaded circles. Silicon atoms ≡Si— in the bulk of the SiO_2 are bonded to three oxygen atoms. Silicon atoms ≡Si— at the interface are bonded to three substrate silicon atoms.

The bond-strained gradient (BSG) (Grunthaner *et al.*, 1979b) model explains the generation of N_{it} by migration of nonbridging oxygen defects resulting from the bond rupture in the strained region of the SiO_2/Si interface ($\sim$3–5 nm) to the border of this interface. Trivalent silicon atoms formed by these defects react as interface states (see Section 3.3.4). It was found that the presence of OH groups enhances defect migration. This model is supported by the interfacial mechanical stress model (Chin and Ma, 1983; Zeheriya and Ma, 1984a,b,c; Kasama *et al.*, 1986). Time, field and temperature dependence of the generation of N_{it} after irradiation cannot be sufficiently explained by these models.

The extrinsic defects in the SiO_2 related to hydrogen have a strong implication for the buildup of N_{it}. Two models deal with the reaction of atomic hydrogen at the SiO_2 interface.

The model introduced by McLean (1980) describes the delayed generation process of N_{it} by the reaction of the *positive charged hydrogen* H^+ with defects at the SiO_2/Si interface. The field dependence of the delayed generation process is related to the positive charged hydrogen H^+. This model is supported by many other experiments (Saks and Brown, 1989, 1990; Saks *et al.*, 1991; Brown and Saks, 1991) (see Fig. 10).

The second model proposed by Griscom (1985) is based in the diffusion of *neutral hydrogen* H^0, which reacts at the SiO_2/Si interface with the Si—H defects. This reaction requires an electron from the Si substrate. The field dependence of this generation is related to the availability of substrate electrons (see Fig. 10).

3.3.8. Summary and discussion. The buildup of oxide charges as well as the prompt and delayed generation of interface states have been a substantial part of research activities since more than 20 years. A satisfactory model which is able to explain all observations and interactions in this context has not been found up to now. The reason for this is the very complex interaction of radiation with the noncrystalline structure of the SiO_2 and its interfaces. Interactions of electronic trapping with chemical reactions of hydrogen related defects and their diffusion, combined with the flexible structure of vitreous silicon dioxide, cannot be compressed into one universal model. According to a picture developed by Griscom *et al.* (1988), the three models discussed above are visualized in Fig. 10. A fraction of e–h pairs generated by radiation recombines and forms excitons which recombine or create electron traps by breaking Si—OH bonds (Si—OH $\Rightarrow$ Si—O$^\cdot$ + H^0). Under the influence of the electric field, the remaining e–h pairs are separated and the electrons move to the positive interface. The electrons are able to break Si—OH bonds and then they are trapped in the Si—O^- defect, releasing an atomic hydrogen. The holes move via polaron hopping processes to the negative interface. Some of the holes are trapped in E' centers or hydrogen related defects to form N_{ot} and another part reacts with hydrogen related defects like Si—H at the interface, creating interface states N_{it}.

Depending on the defect density of the SiO_2 or in other words, the radiation hardness of the oxide, most of the holes reach the SiO_2/Si interface and recombine with substrate electrons. Time dispersive polaron transport is described by the CTRW model. The interactions of the polaron model are denoted by the dotted area in Fig. 10.

Reactions with Si—H or Si—OH defects release atomic hydrogen H^0 which can recombine with another H^0 to form molecular H_2 or react with a polaron to form H^+. This hydrogen is responsible for the delayed generation of N_{it}. Neutral hydrogen moves to the SiO_2/Si interface by diffusion, and the positive charged hydrogen by diffusion and field assistance drift. In both cases electrons are needed for the reaction at the interface to form dangling bonds (P_b-centers). Reverse reactions of the atomic and molecular hydrogen with defects of the SiO_2 must be included in the reaction model. Time dependent post-irradiation buildup of N_{it} caused by neutral hydrogen is defined by a combination of diffusion and an nth-order ($n = 2$–3) chemical reaction of H^0 with the SiO_2 (Griscom, 1985; Brown, 1985). The time dispersive transport of the positive charged hydrogen H^+ is explained by a CTRW model (Brown and Saks, 1991) with slightly different parameters compared to the hole transport:

	hydrogen ions H^+	polaron h
disorder parameter α	0.38	0.15
hopping distance a	3.3 nm	1 nm
activation energy E_a	0.8 eV	0.64–0.75 eV
field dependence	$\sim E^{-1.75}$	$\sim \exp((\Delta_0 - b \cdot E_{ox})/kT)$
oxide thickness dependence of t_r	$\sim d_{ox}^{2.6}$	$\sim d_{ox}^4$.

Buildup of N_{ot} and N_{it} caused by ionizing radiation and their post-irradiation annealing behaviour is a very complex process depending on the MOS technology, radiation type and energy, dose rate, bias condition during and after irradiation, and temperature. The large number of parameters is a limiting factor in devising a simple model to predict the radiation hardness of MOS devices.

3.4. *Radiation effects on MOS devices and circuits*

Basic effects of ionizing radiation on MOS structures have been discussed in the previous sections. These primary effects of trapped oxide charges and generated interface states cause the following changes in MOS transistor characteristics and CMOS device performance:

MOS transistor:

—negative threshold voltage shift	ΔV_{th}
—decrease of the surface mobility	μ_0
—increase of surface recombination velocity	S_0
—decrease of the transconductance	g_m
—increase of source drain leakage current	I_L
—decrease of drain to source breakdown voltage	V_{BR}
—increase of noise	N

CMOS circuits:

—decrease of the output voltage	V_{out}
—decrease of max. output current	I_{os}
—increase of propagation delay time	t_p
—increase of the quiescent current	I_{DD}

Total dose response of the threshold voltage shift of N- and P-channel transistors due to the number of trapped charges N_{ot} and generated interface states N_{it} is different, as shown in Fig. 11. Provided that the total amount of charges is trapped at the SiO_2/Si interface, the threshold voltage shift ΔV_{Th} can be defined as follows:

$$\Delta V_{Th} = -\frac{d_{ox} \cdot q}{\epsilon_{SiO_2}} \cdot (\Delta N_{ot} \pm \Delta N_{it}) \qquad (41)$$

with the permittivity of silicon dioxide being ϵ_{SiO_2}, the elementary charge q and the oxide thickness d_{ox}.

The threshold voltage shift is proportional to the number of trapped oxide charges and the number of charged interface states. The fermi level controls the charge state of the N_{it}. In the case of the N-channel transistor, the interface states are negatively charged (acceptor states in upper half of the band gap) and therefore the minus sign in equation (41) is valid. For P-channel transistors, the interface states are positive charged (donator states in the lower half of the band gap) and must be added to the oxide charge (plus sign). Therefore, under the same test conditions, the threshold voltage shift of P-channel transistors is stronger compared to the shift of N-channel transistors.

If the magnitude of ΔV_{Th} of the P-channel transistor reaches the supply voltage, the transistor cannot be switched into the *on*-state, which leads to functional failure.

Negative threshold voltage shift of the N-channel transistor turns the transistor on. This increases the leakage current and the transistor cannot be switched into the *off*-state, thus generating function failures. For the N-channel transistor, the balance of ΔN_{ot} and ΔN_{it} leads to a turn around effect of ΔV_{Th} (Fig. 11). This so called *rebound* (Schwank *et al.*, 1984) or *superrecovery effect* (Johnston, 1984) can increase the threshold voltage above its pre-irradiation value.

The mobility degradation μ_i is related to the Coulomb scattering by trapped charges (Sun and Plummer, 1980; Galloway *et al.*, 1984, 1985; Sexton and Schwank, 1985; Soppa and Wagemann 1980; Zupac *et al.*, 1992). The reduction of μ_0 was first fitted only by the interface state density (Sexton and Schwank, 1985), but recent work include the trapped oxide charges as well (Soppa and Wagemann, 1980; Zupac *et al.*, 1992).

$$\mu_i = \frac{\mu_0}{1 + \alpha_{it} \cdot \Delta N_{it} \cdot \alpha_{ot} \cdot \Delta N_{ot}} \qquad (42)$$

with the fitting values being $\alpha_{it} = 3.9 \cdot 10^{-12}\,cm^2$ and $\alpha_{ot} = 0.7 \cdot 10^{-12}\,cm^2$ at 300 K and $\alpha_{it} = 3.4 \cdot 10^{-12}\,cm^2$ and $\alpha_{ot} = 1.3 \cdot 10^{-12}\,cm^2$ at 77 K (Zupac *et al.*, 1992).

Transconductance g_m, cut off frequency F_T and the output short current I_{os} is proportional to the surface mobility μ_i. Also the increase of the propagation delay t_p time of a CMOS inverter is related to the mobility degradation due to the reduction of I_{os} (Sexton and Schwank, 1985).

$$\frac{\Delta t_p}{C_{load}} = \frac{0.5 \cdot V_{out}}{I_{os}} \quad \text{with } V_{out} = V_{DD} - 0.5 \qquad (43)$$

where V_{out} is the maximum output voltage, V_{DD} the drain voltage and C_{load} the load capacitor of the circuit.

The generation of N_{it} increases surface recombination velocity S_0 (Galloway *et al.*, 1985; Sexton and Schwank, 1985; Eades and Swanson, 1985). This characteristic is important for the storage time of CCD and DRAM. S_0 is proportional to N_{it} and the square root of the product of the hole and electron capture cross sections σ_n, σ_h:

$$S_0 = 0.5 \cdot (\sigma_n \cdot \sigma_h)^{1/2} \cdot \upsilon \cdot kT \cdot N_{it} \qquad (44)$$

where v is the thermal velocity.

The dominant radiation effect on CMOS technologies is the subthreshold leakage current of the N-channel transistor (Winokur *et al.*, 1984, 1986), and for nonradiation hard technologies the parasitic leakage path between source and drain at the bird's beak (Oldham *et al.*, 1987). Parasitic field oxide

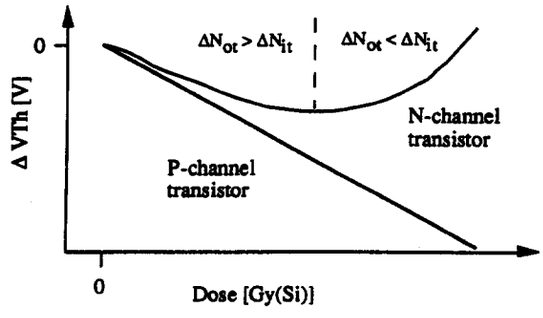

Fig. 11. Schematic threshold voltage shift ΔV_{Th} of N- and P-channel transistors versus absorbed dose.

Table 4. Sensitivity and damage behaviour of device families

	Total dose	Displacement	SEP (0 = not, 3 = very sensitive)	
Diodes				
Rectifier	1	1	0	Recombination and generation increase. Breakdown voltage slightly increases. At very high fluencies series resistances become pronounced.
Switching diode	1	1	0	The switching is even faster. No severe limitation.
Voltage reference	0	1	0	If temperature compensated, the temperature coefficient changes to positive sign. Zener-voltage increases or decreases.
Transistors				
Bipolar NF	3	3	0	Very sensitive, especially at low currents. Current gain decreases. Leakage currents increase by orders of magnitude.
HF	1	1	0	Less vulnerable compared to NF-transistor. High transit frequencies are advantageous.
Microwave	1	1	0	Thinning the base of the transistor gains hardness.
Power	3	3	2	Very sensitive, especially at low currents. Both emitter yield and base transport factor degrade heavily. SEP may cause destructive failure.
JFET	1	1	0	Si and GaAs-FETs (J- and MES-) are commonly hard against all kind of damage, probably except for SEP.
MOSFET	3	0	1	Very sensitive to total dose, pMOS is partly harder than nMOS. Due to its anomalous annealing behaviour (rebound effect) the nMOS degradation is the less predictable. For n- and pMOS threshold voltage shifts to more negative values and leakage currents increase by orders of magnitude.
OPTO electronic				
LED	0	2	0	GaAs is relatively hard, but the creation of non radiative centers limit the light output. Lenses darken.
Photo transistor	3	3	2	Very sensitive. Photo-sensitivity decreases very rapidly.
Opto coupler	3	3	2	Combination of LED and phototransistor deteriorates even worse compared to individual components.
Solar cell	0	2	0	Very sensitive against displacement which reduces the diffusion length and thus the efficiency especially in the long wave length region.
Optical waveguide	3	1	0	Extremely sensitive due to darkening. But hardened fibers are available.
CCD	3	1	3	Most sensitive devices, especially when they are operated at cryostatic temperatures. Slight improvement by using buried channel CCDs.
Linear IC				
OpAmp	3	3	2	Very sensitive but hardened OpAmps are available. The sensitivity is caused by low current operation, matching properties and d.c.-coupling.
Comparator	3	2	2	Sensitive, large failure range, depending on technology.
Reference source	2	2	1	Sensitive.
Digital IC				
TTL/ECL	1	1	0	Hard technology due to fast transistors, ECL even harder than TTL.
LSTTL	1	1	0	As TTL with minor deterioration.
CMOS/HCMOS	3	0	2	The commercial CMOS and HCMOS parts are the most vulnerable technology for total dose (only CCDs are more sensitive). The failure mechanism is alike n- and pMOS. Sensitive to SEP
CMOS (rad hard)	1	0	2	Changes in technology and layout improve the performance to up to 1 to 10 kGy. Very expensive.
SOS (rad hard)	1	0	0	Alike CMOS (rad hard). Design rules are known to almost suppress SEPs.
GaAs	1	1	1	Very hard against displacement and total dose. Due to their fast operation, they are sensitive to SEP.
HMOS	3	0	3	Very sensitive, but hardened devices are available.
EPROMS	3	1	3	Very sensitive due to decharging of information. The same is true for SEP. At higher doses the tunnel characteristic of the SiO_2-layer is degraded.

leakage is also significant for the radiation hardness of advanced bipolar technologies using recessed field oxide or walled emitter structures (Pease *et al.*, 1983, 1985; Buschbom *et al.*, 1983; Wulf *et al.*, 1990).

3.5. Irradiation qualification tests

In the previous sections the basic effects of ionizing radiation on MOS devices have been briefly discussed. Many phenomena are in general understood, but the details are still part of research programs. The impact of processing steps on the radiation hardness of devices and circuits is not completely under control. Irradiation qualification tests must always be performed to verify the radiation hardness of a technology. For space applications many different device types from various technologies and manufacturers are used. Many evaluation and qualification tests have been performed over recent years. Depending on the properties of the device and the technology used radiation sensitivity is related to displacement damage and/or total dose effects. Irradiation tests must consider the dominant degradation effect of device types and technologies. The relative sensitivity due to the degradation effects is summarized in Table 4 (Boden *et al.*, 1990; Bennemann *et al.*, 1990). The complex interdependencies of the radiation response of electronic devices depend on the following facts:

—type of radiation (Dozier *et al.*, 1987);

—dose rate (Schwank *et al.*, 1984, 1989; Johnston, 1984; Winokur *et al.*, 1986, 1987; Schrimpf *et al.*,

Table 5. Total dose failure of various technologies and device families.

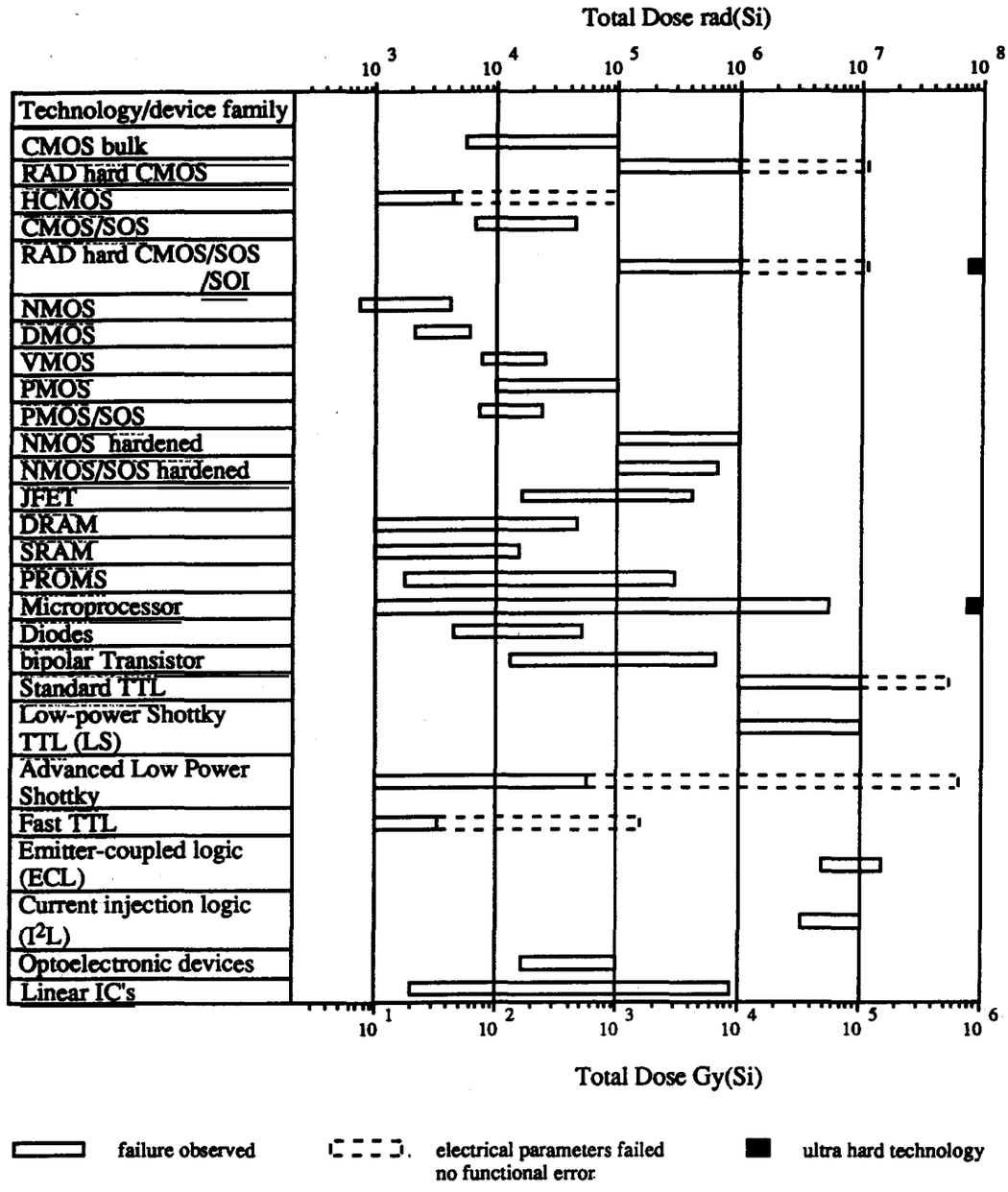

The left margin of the bars indicates the *first* observed failure and the right margin the highest dose level at which *all* devices failed.

1988; Fleetwood *et al.*, 1988, 1989, 1991; Enlow *et al.*, 1991);

—bias condition during and after irradiation (Dressendorfer *et al.*, 1981; Boden *et al.*, 1990; Fleetwood *et al.*, 1987, 1990);

—ambient temperature during irradiation (Pease *et al.*, 1983);

—annealing time and temperature (Schwank *et al.*, 1984; Oldham *et al.*, 1987; Fleetwood *et al.*, 1988);

—packaging (Kohler *et al.*, 1988);

—technology (Dressendorfer, 1989; Winokur *et al.*, 1985);

—layout and circuit design (Dressendorfer, 1989).

Therefore a well defined irradiation test plan is required (Bräunig *et al.*, 1982; MIL HDBK-279, 1985).

Standardizations of the test procedures for total dose testing are defined by MIL Standard Method 1019.4 (MIL-STD-833C) or ESA/SCC 22900. This provides the opportunity to compare irradiation test results from different test facilities. These

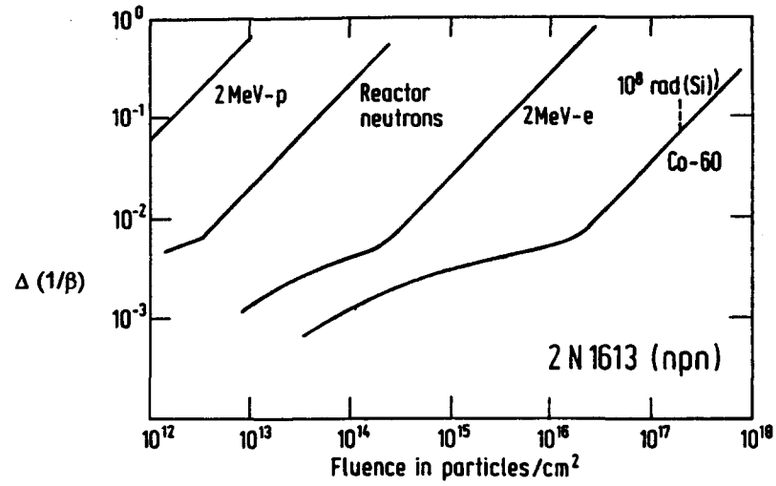

Fig. 12. Change in reciprocal current gain as function of the fluence for different radiation species.

specifications are continually updated to the implication of technology changes, and the new understanding of the radiation response (Fleetwood *et al.*, 1989; Brown and Johnston, 1987). A critical point is the delayed generation of interface states and the annealing behaviour of oxide charges. Radiation hard MOS devices show a different prompt and delayed response from nonradiation hard devices. Nonradiation hard devices degrade dominantly by hole trapping in the gate and the field oxide. Dose rate dependence of nonradiation hard devices is smaller compared with radiation hard devices (Fleetwood *et al.*, 1989). Delayed generation of interface states is more pronounced in radiation hard devices, leading to rebound and superrecovery effects. These effects cannot be observed in short time annealing after irradiation at RT. High temperature annealing at 100°C over a period of 168 h with the same bias condition as used during irradiation has been recommended (Fleetwood *et al.*, 1989).

A new approach to radiation hardness assurance prediction is the qualified manufacturer list (QML) methodology (Winokur *et al.*, 1990; Alexander, 1990) as described by Pease and Alexander (1994).

Total dose failure levels of relevant technologies and device families are summarized in Table 5. This review of the sensitivity of the various technologies and device families shows the range at which the *first* failure has been observed (left margin of the bars) to the highest level at which *all* devices failed (right margin of the bars). This Table 5 contains irradiation test results from various test facilities published in recent years (Long, 1981; Wulf *et al.*, 1981–1990; Leray *et al.*, 1990; IEEE, 1970–1990).

4. MISCELLANEOUS EFFECTS

As already pointed out, many semiconductor devices experience a mixed damage behaviour, that means, they suffers from both displacement damage and TID. As a result, damage depends on the ionising and displacing nature of the radiation species under consideration. For instance an electron delivers most of its energy by ionisation, a proton can be equally damaging by both degradation types and a neutron is only slightly ionising, but predominantly displacing. Figure 12 illustrates this behaviour for the current gain degradation of an npn-transistor (Brown, 1964). Here different radiation species are used to demonstrate the relative importance of displacement damage and TID. Depending on the ionising nature of the radiation species at lower particle fluencies the saturating damage by TID is evident and at higher fluencies, according to the damage factor concept, a linear change of reciprocal gain and fluence is seen. The different onset of the latter behaviour is reflected by the different ratio of displacement to ionisation energy loss. There is a clear order from 2 MeV-protons, 1 MeV-neutrons, 2 MeV-electrons to Co-γ-rays.

In equation (15) the third term describes the influence of the surface in terms of the surface recombination velocity s. The interface between the silicon and the passivating oxide of a planar transistor, for instance, is influenced by ionising radiation, as seen in Section 3, by the generation of oxide charges and interface states. Bipolar devices are commonly doped to a higher surface concentration and this reduces the effect of the fixed charges but the surface recombination velocity is altered by interface states and this in turn enhances leakage currents just at the interface. In general, the surface mobility of the free carriers is reduced. This mixed behaviour can be observed in a variety of devices.

REFERENCES

Aitken J. M. and Young D. R. (1977) Avalanche injection of the holes into SiO_2. *IEEE Trans. Nucl. Sci.* **NS-24**, 2128.

Alexander D. R. (1990) Implication of qualified manufacturers list reliability procedures for radiation hardness assurance. *Nucl. Space Radiation Effects Conference*, Short Course, Reno, NV.

ASTM Standard E170 (1985) Standard terminology relating to radiation measurements and dosimetry. *1985 Annual book of ASTM Standards, Vol. 12.02, Nuclear II, Solar and Geothermal Energy*, p. 25. American Society for Testing and Materials, Philadelphia, PA.

ASTM Standard E665. Standard practice for determining absorbed dose versus depth in materials exposed to X-ray output of flash X-ray machines. *ASTM Standards, Vol. 12.02: Nuclear (II), Solar and Geothermal Energy*, pp. 299–5400. American Society for Testing and Materials, Philadelphia, PA.

ASTM Standard E666. Standard practice for calculation of absorbed dose from gamma or X radiation. *ASTM Standards, Vol. 12.02: Nuclear (II), Solar and Geothermal Energy*, pp. 299–5400. American Society for Testing and Materials, Philadelphia, PA.

ASTM Standard E668. Standard practice for application of thermoluminescence-dosimeter (TLD) systems for determining absorbed dose in radiation-hardness testing of electronic devices. *ASTM Standards, Vol. 12.02: Nuclear (II), Solar and Geothermal Energy*, pp. 299–5400. American Society for Testing and Materials, Philadelphia, PA.

Ausman G. A. (1986) Field dependence of geminate recombination in a dielectric medium. Harry Diamond Laboratories Report No. 2097, Adelphi, MD.

Ausmann G. A. Jr and McLean F. B. (1975) Electron–hole pair creation energy in SiO_2. *Appl. Phys. Lett.* **26,** 173.

Balk P. (1965) *Extended Abstracts of Electronics Division*, Vol. 14, Abstr. 109, p. 237. The Electrochemical Society, Princeton; Spring Meeting, San Francisco.

Barry A. L., Lehmann B., Fritsch D. and Bräunig D. (1991) Energy dependence of electron damage and displacement threshold energy in 6C silicon carbide. *IEEE Trans. Nucl. Sci.* **38,** 1111.

Bäuerlein R. (1968) Strahlenschäden in Halbleitern und Halbleiter-Bauelementen. In *Festkörperprobleme VIII* (Edited by Madelung O.). Pergamon Press, Oxford.

Benedetto J. M. and Boesch H. E. Jr (1986) The relationship between Co-60 and 10 keV X-ray damage in MOS devices. *IEEE Trans. Nucl. Sci.* **NS-33,** 1318.

Bennemann A., Boden A., Bräunig D., Brumbi D., Klein J. W., Schott J. U., Seifert C. Ch., Spillekothen H.-G. and Wulf F. (1990) The effects of radiation on electronic devices and circuits. *Kerntechnik* **55,** 261.

Boden A., Wulf F. and Bräunig D. (1990) Irradiation tests and radiation hardness prediction considerations on electronic components for space application. In *Proc. ESA Electronic Components Conference*, ESTEC Noordwijk, ESA SP-313, p. 413.

Boesch H. E. Jr, McGarrity J. M. and McLean F. B. (1978) Temperature and field-dependent charge relaxation in SiO_2 gate insulators. *IEEE Trans. Nucl. Sci.* **NS-25,** 1012.

Boesch H. E. Jr, McLean F. B., Benedetto J. M. and McGarrity J. M. (1986) Saturation of the threshold voltage shift in MOSFET's at high total dose. *IEEE Trans. Nucl. Sci.* **NS-33,** 1191.

Boesch H. E. Jr, McLean F. B., McGarrity J. M. and Ausmann G. A. Jr (1975) Hole transport and charge relaxation in irradiated SiO_2 MOS-capacitors. *IEEE Trans. Nucl. Sci.* **NS-22,** 2163.

Boesch H. E. Jr, McLean F. B., McGarrity J. M. and Winokur P. S. (1985) Enhanced flatband voltage recovery in hardened thin MOS capacitors. *IEEE Trans. Nucl. Sci.* **NS-32,** 3940.

Bragg W. H. and Kleeman R. D. (1906) On the recombination of ions in air and other gases. *Phil. Mag.* **12,** 273.

Bräunig D. (1989) *Wirkung hochenergetischer Strahlung auf Halbleiterbauelemente*. Springer, Berlin.

Bräunig D., Wulf F., Gaebler W. and Boden A. (1982) Irradiation test guidelines for radiation hardness of electronic components. DLVLR Test Report TN 53/10 and HMI Test Report, HMI-B380.

Brown D. B. (1980) Photoelectron effects on the dose deposition in MOS devices caused by low energy X-ray sources. *IEEE Trans. Nucl. Sci.* **NS-27,** 1465.

Brown D. B. (1985) The time dependence of interface state production. *IEEE Trans. Nucl. Sci.* **NS-32,** 3900.

Brown D. B. and Dozier C. M. (1981) Electron–hole recombination in irradiated SiO_2 from a microdosimetry viewpoint. *IEEE Trans. Nucl. Sci.* **NS-28,** 4142.

Brown D. B. and Johnston A. H. (1987) A framework for an integrated set of standards for ionizing radiation testing of microelectronics. *IEEE Trans. Nucl. Sci.* **NS-34,** 1720.

Brown D. B. and Saks N. S. (1991) Time dependence of radiation-induced interface trap formation in metal–oxide-semiconductor devices as a function of the oxide thickness and applied field. *J. Appl. Phys.* **70,** 7434.

Brown R. R. (1964) Proton and electron permanent in silicon semiconductor devices. Boeing report D2-90570.

Brucker G. J. (1981) Exposure dose-rate-dependence for a CMOS/SOS memory. *IEEE Trans. Nucl. Sci.* **NS-28,** 4056.

Burke E. A. and Garth J. C. (1976) An algorithm for energy deposition at interfaces. *IEEE Trans. Nucl. Sci.* **NS-23,** 1838.

Buschbom M. L., Jeffry E. N., Rhine L. E. and Spratt D. B. (1983) Gamma total dose effects on ALS bipolar oxide sidewell isolated devices. *IEEE Trans. Nucl. Sci.* **NS-30,** 4105.

Chadsy W. L. (1978) X-ray dose enhancement. *IEEE Trans. Nucl. Sci.* **NS-25,** 1591.

Chang S. T. and Lyon S. A. (1986) Location of the positive charge trapped near the Si–SiO_2 interface at low temperature. *Appl. Phys. Lett.* **48,** 136.

Chin M. R. and Ma T. P. (1983) Gate-width dependence of radiation-induced interface traps in metal/SiO_2/Si devices. *Appl. Phys. Lett.* **42,** 883.

Clement J. J. (1978) A study of radiation effects in MOS capacitors. Ph.D. Dissertation, Princeton University.

Corbett J. W. and Bourgoin J. C. (1975) In *Point Defects in Solids* (Edited by Crawford J. H. and Slifkin L. F.). Plenum Press, New York.

Crabb R. L. (1994) Solar cell radiation damage. *Radiat. Phys. Chem.* **43,** 93.

Curtis D. L. Jr and Srour J. R. (1977) The multiple-trapping model transport in SiO_2. *J. Appl. Phys.* **49,** 3819.

Curtis O.L., Srour J. R. and Chiu K. Y. (1974) Hole and electron transport in SiO_2 films. *J. Appl. Phys.* **45,** 4506.

Dale C. J., Marshall P. W., Burke E. A., Summers G. P. and Bender G. E. (1989) The generation lifetime damage factor and its variance. *IEEE Trans. Nucl. Sci.* **NS-36,** 1872.

Derbenwick G. F. and Sander H. H. (1977) CMOS Hardness prediction for low-dose-rate environments. *IEEE Trans. Nucl. Sci.* **NS-24,** 2244.

Di Maria D. J. (1976) Determination of insulator bulk trapped charges and centroids from photocurrent-voltage characteristics of MOS structures. *J. Appl. Phys.* **47,** 4073.

Di Maria D. J. and Stasiak J. W. (1989) Trap creation in silicon dioxide produced by hot electrons. *J. Appl. Phys.* **65,** 2342.

Di Maria D. J., Feigl F. J. and Butler S. R. (1975) Capture and emission of electrons at 2.4 eV-deep trap level in SiO_2 films. *Phys. Rev. B* **11,** 5023.

Dozier C. M. and Brown D. B. (1980) Photon energy dependence of radiation effects in MOS structures. *IEEE Trans. Nucl. Sci.* **NS-27,** 1694.

Dozier C. M. and Brown D. B. (1981) Effect of photon energy on the response of MOS devices. *IEEE Trans. Nucl. Sci.* **NS-28,** 4137.

Dozier C. M. and Brown D. B. (1983) The use of low energy

X-rays for device testing—a comparison with Co-60 irradiation. *IEEE Trans. Nucl. Sci* **NS-30,** 4382.

Dozier C. M., Fleetwood D. M., Brown D. B. and Winokur P. S. (1987) An evaluation of low-energy X-ray and cobalt-60 irradiations of MOS transistors. *IEEE Trans. Nucl. Sci.* **NS-34,** 1535.

Dressendorfer P. V. (1989) Radiation effects on MOS devices and circuits. In *Ionizing Radiation Effects in MOS Devices and Circuits* (Edited by Ma T. P. and Dressendorfer P. V.), p. 256. Wiley, New York.

Dressendorfer P. V. (1989) Radiation-hardening technology. In *Ionizing Radiation Effects in MOS Devices and Circuits* (Edited by Ma T. P. and Dressendorfer P. V.), p. 333. Wiley, New York.

Dressendorfer P. V., Soden J. M., Harrington J. J. and Nordstrom T. V. (1981) The effects of test conditions on radiation hardness results. *IEEE Trans. Nucl. Sci.* **NS-28,** 4281.

Eades W. D. and Swanson R. M. (1985) Calculation of surface generation and recombination velocities at the Si–SiO_2 interface. *J. Appl. Phys.* **58,** 4267.

Enlow E. W., Pease R. L. Combs W., Schrimpf R. D. and Nowlin R. N. (1991) Response of advanced bipolar processes to ionizing radiation. *IEEE Trans. Nucl. Sci.* **NS-38,** 1342.

ESA/SCC Basic Specification No. 22900. Total dose steady-state irradiation test method.

Evans R. D. (1955) *The Atomic Nucleus.* McGraw-Hill, New York.

Ferry D. K. (1979) Electron transport and breakdown in SiO_2. *J. Appl. Phys.* **50,** 1422.

Fister G. and Scher H. (1978) Dispersive (non-gaussian) transient transport in disordered solid. *Adv. Phys.* **27,** 747.

Fleetwood D. M. and Winokur P. S. (1988) Effect of bias on the response of metal–oxide-semiconductor devices to low-energy X-ray and cobalt-60 irradiation. *Appl. Phys. Lett.* **52,** 1514.

Fleetwood D. M., Dressendorfer P. V. and Turpin D. C. (1987) A reevaluation of worst-case postirradiation response for hardened MOS transistors. *IEEE Trans. Nucl. Sci.* **NS-34,** 1178.

Fleetwood D. M., Winokur P. S. and Meisenheimer T. L. (1991) Hardness assurance for low-dose space applications. *IEEE Trans. Nucl. Sci.* **NS-3,** 1552.

Fleetwood D. M., Winokur P. S. and Riewe L. C. (1990) Prediction switched-bias response from steady-state irradiation. *IEEE Trans. Nucl. Sci.* **NS-37,** 1806.

Fleetwood D. M., Winokur P. S. and Schwank J. R. (1988) Using laboratory X-ray and Co 60 irradiation to predict CMOS device repsonse in strategic and space environments. *IEEE Trans. Nucl. Sci.* **NS-35,** 1497.

Fleetwood D. M., Winokur P. S., Riewe L. C. and Pease R. L. (1989) An improved standard total dose test for CMOS space electronics. *IEEE Trans. Nucl. Sci.* **NS-36,** 1963.

Fleetwood D. M., Beutler D. E., Lorence L. J. Jr, Brown D. B., Draper B. L., Riewe L. C., Rosenstock H. B. and Knott D. P. (1988) Comparison of enhanced device response and predicted X-ray dose enhancement effects on MOS oxides. *IEEE Trans. Nucl. Sci.* **NS-35,** 1265.

Freeman R. and Holmes-Siedle A. (1978) A simple model for predicting radiation effects in MOS devices. *IEEE Trans. Nucl. Sci.* **NS-25,** 1216.

Galloway K. F., Gaitan M. and Russel T. J. (1984) A simple model for separating interface and oxide charge effects on MOS device characteristics. *IEEE Trans. Nucl. Sci.* **NS-31,** 1497.

Galloway K. F., Wilson C. L. and Witte L. C. (1985) Charge-sheet model to extract radiation-induced oxide and interface charge. *IEEE Trans. Nucl. Sci.* **NS-32,** 3975.

Garth J. C. (1986) An algorithm for calculation dose profiles in multi-layered devices using a personal computer. *IEEE Trans. Nucl. Sci.* **NS-33,** 1266.

Garth J. C., Chadsy W. L. and Sheppard R. L. (1975) Monte Carlo analysis of dose profiles near photon irradiated material interfaces. *IEEE Trans. Nucl. Sci.* **NS-22,** 2562.

Griscom D. L. (1985) Diffusion of radiolytic molecular hydrogen as a mechanism for the post-irradiation buildup of interface states in SiO_2-on-Si structures. *J. Appl. Phys.* **58,** 2524.

Griscom D. L. and Friebele E. J. (1982) Effects of ionizing radiation on amorphous insulators. *Radiat. Effects* **65,** 63.

Griscom D. L., Brown D. B. and Saks N. S. (1988) Nature of radiation-induced point defects in amorphous SiO_2 and their role in SiO_2-on-Si structures. In *The Physics and Chemistry of SiO_2 and the Si–SiO_2 Interface* (Edited by Helms C. R. and Deal B. E.), p. 295. Plenum Press, New York.

Grunthaner F. J. and Maserjian J. (1978) Chemical structure of the transitional region of the SiO_2/Si interface. In *The Physics of the SiO_2 and its Interfaces* (Edited by Pandalides S.), p. 389. Pergamon Press, New York.

Grunthaner F. J., Grunthaner P. J. and Maserjian J. (1982) Radiation-induced defects in SiO_2 as determined with XPS. *IEEE Trans. Nucl. Sci.* **NS-29,** 1462.

Grunthaner F. J., Grunthaner P. J., Vasquez R. P., Lewis B. F., Maserjian J. and Madhukar A. (1979) Local atomic and electronic structure of oxide/GaAs and SiO_2/Si interfaces using high-resolution XPS. *J. Vac. Sci. Technol.* **16,** 1443.

Grunthaner F. J., Grunthaner P. J., Vasquez R. P., Lewis B. F., Maserjian J. and Madhukar A. (1979b) High-resolution X-ray photoelectron spectroscopy as a probe of local atomic structure: application to amorphous SiO_2 and the Si–SiO_2 interface. *Phys. Rev. Lett.* **43,** 1683.

Habing D. H. and Shafer B. D. (1973) Room temperature annealing of ionization-induced damage in CMOS circuits. *IEEE Trans. Nucl. Sci.* **NS-20,** 307.

Hamm R. N. (1986) Dose calculations for Si–SiO_2 layered structures irradiated by X-rays and Co-60 gamma rays. *IEEE Trans. Nucl. Sci.* **NS-33,** 1236.

Hu G. (1980) Study of the generation of interface states in the Si–SiO_2 system after high field stress and after X-irradiation. Ph.D. Dissertation, Princeton University.

Hubbell J. H. (1969) Photon cross section, attenuation coefficient and energy absorption coefficients from 10 keV to 100 keV. *U.S. Department of Commerce, Natioanl Bureau of Standards Handbooks*, NSRDS-NBS 29.

Hughes R. C. (1973) Charge-carrier transport phenomena in amorphous SiO_2: direct measurement of the drift mobility and lifetime. *Phys. Rev. Lett.* **30,** 1333.

Hughes R. C. (1975a) Hot electrons in SiO_2. *Phys. Rev. Lett.* **35,** 449.

Hughes R. C. (1975b) Hole mobility and transport in thin SiO_2 films. *Appl. Phys. Lett.* **26,** 436.

Hughes R. C. (1977) Time-resolved hole transport in Si–SiO_2. *Phys. Rev.* **B15,** 2012.

Hughes R. C. (1978) High field electronic properties of SiO_2. *Solid-State Electron.* **21,** 251.

Hughes G. W. and Powel R. J. (1976) MOS hardness characterization and its dependence upon some process and measurement variables. *IEEE Trans. Nucl. Sci.* **NS-23,** 1569.

Hughes R. C., Eernisse E. P. and Stein H. J. (1975) Hole transport in MOS oxides. *IEEE Trans. Nucl. Sci.* **NS-22,** 2227.

ICRU report 33 (1980) International commission on radiation units and measurements, radiation quantities and units. Bethesda, MD.

IEC 544-1. *Guide for Determining the Effects of Ionizing Radiation on Insulating Materials. Part 1: Radiation Interaction and Dosimetry.*

IEEE (1970–1990) IEEE Annual Conference on Nuclear and Space Radiation Effects. *IEEE Trans. Nucl. Sci.* **NS-17–NS-37.**

Jaffe G. (1913) Zur Theorie der Ionisation in Kolonnen.

Ann. Phys. Leipzig **42,** 303; reprinted in 1914 in *Phys. Z.* **15,** 353; in 1929 in *Phys. Z.* **23,** 849.

Johnston A. H. (1984) Super recovery of total dose damage in MOS devices. *IEEE Trans. Nucl. Sci.* **NS-31,** 1427.

Kasama K., Toyokawa F., Tsukiji M., Sakamoto M. and Kobayashi K. (1986) Mechanical stress dependence of radiation effects in MOS structures. *IEEE Trans. Nucl. Sci.* **NS-33,** 1210.

Kellerer A. M. (1985) Fundamentals of microdosimetry. In *Dosimetry of Ionizing Radiation*, Vol. 1. Academic Press, New York.

Kim Y. Y. and Lenahan P. M. (1988) Electron-spin-resonance study of radiation-induced paramagnetic defects in oxides grown on (100) silicon substrates. *J. Appl. Phys.* **64,** 3551.

Kohler R. A., Kushner R. A. and Lee K. H. (1988) Total dose radiation hardness of MOS-devices in hermetic ceramic packages. *IEEE Trans. Nucl. Sci.* **NS-35,** 1492.

Lai S. K. (1983) Interface trap generation in silicon dioxide when electrons are captured by trapped holes. *J. Appl. Phys.* **54,** 2540.

Lakshmanna V. and Vengurlekar A. S. (1988) Logarithmic detrapping response for holes injected into SiO_2 and influence of the thermal activation and electric field. *J. Appl. Phys.* **63,** 4248.

Langevin M. P. (1903a) L'ionization des gaz. *Ann. Chim. Phys.* **28,** 289.

Langevin M. P. (1903b), Recombination et mobilities des ions dans les gaz. *Ann. Chim. Phys.* **28,** 433.

Lehmann B., Bräunig D. (1993) A DLTS variation for the determination of displacement threshold energies in GaAs. *J. Appl. Phys.* Submitted.

Lelis A. J., Oldham T. R., Boesch H. E. Jr and McLean F. B. (1989) The nature of the trapped-hole annealing process. *IEEE Trans. Nucl. Sci.* **NS-36,** 1808.

Lenahan P. M. and Dressendorfer P. V. (1982) Effect of bias on radiation-induced paramagnetic defects at the silicon–silicon dioxide interface. *Appl. Phys. Lett.* **41,** 542.

Lenahan P. M. and Dressendorfer P. V. (1983a) Microstructural variations in radiation hard and soft oxides observed through electron spin resonance. *IEEE Trans. Nucl. Sci.* **NS-30,** 4602.

Lenahan P. M. and Dressendorfer P. V. (1983b) An electron spin resonance study of radiation-induced electrically active paramagnetic centers at the Si/SiO_2 interface. *J. Appl. Phys.* **54,** 1457.

Lenahan P. M. and Dressendorfer P. V. (1984a) Paramagnetic trivalent silicon centers in gamma irradiated metal–oxide–silicon structures. *Appl. Phys. Lett.* **44,** 96.

Lenahan P. M. and Dressendorfer P. V. (1984b) Hole traps and trivalent silicon centers in metal/oxide/silicon devices. *J. Appl. Phys.* **55,** 3495.

Lenahan P. M., Brower, L. L., Dressendorfer P. V. and Johnson W. C. (1981) Radiation induced trivalent silicon defect buildup at the $Si–SiO_2$ interface in MOS structures. *IEEE Trans. Nucl. Sci.* **NS-28,** 4105.

Leray J. L., Dupont-Nivet E., Péré J. F., Coic Y. M., Raffaelli M., Auberton-Hervé A. J., Bruel M., Giffard B. and Margail J. (1990) CMOS/SOI hardening at 100 Mrad(SiO_2). *IEEE Trans. Nucl. Sci.* **NS-37,** 2013.

van Lint V. A. J., Gigas G and Barengoltz J. (1975) Correlation of displacement effects produced by electrons, protons and neutrons. *IEEE Trans. Nucl. Sci.* **22,** 2663.

van Lint V. A. J., Flanagan T. M., Leadon R. E., Naber J. A. and Rodgers V. C. (1980) *Mechanisms of Radiation Effects in Electronic Materials*, Vol. 1. Wiley, New York.

Lipkin L., Reisman A. and Williams C. K. (1990a) Hole trapping phenomena in the gate insulator of As-fabricated insuled gate field effect transistors. *J. Appl. Phys.* **68,** 4620.

Lipkin L, Reisman A. and Williams C. K. (199b) Conservation and filling of neutral traps in SiO_2 during ionizing radiation exposure. *Appl. Phys. Lett.* **57,** 2237.

Long D. M. (1981) Hardness of MOS and bipolar integrated circuits. *IEEE Trans. Nucl. Sci.* **NS-27,** 1674.

McKinley W. A. Jr and Feshbach H. (1948) The Coulomb scattering of relativistic electrons by nuclei. *Phys. Rev.* **74,** 1759.

Manchanda L., Vasi J. and Bhattacharyya A. B. (1981) The nature of intrinsic hole traps in thermal silicon dioxide. *J. Appl. Phys.* **52,** 4690.

McLean F. B. (1976) A direct tunneling of charge transfer at the insulator–semiconductor interface in MIS devices. U.S. Government Report, HDL-TR-1765.

McLean F. B. (1980) A framework for understanding radiation-induced interface states in SiO_2 MOS structures. *IEEE Trans. Nucl. Sci.* **NS-27,** 1651.

McLean F. B. and Ausmann G. A. Jr (1977) Simple approximate solutions to continuous-time-random-walk transport. *Phys. Rev. B* **15,** 1052.

McLean F. B. and Oldham T. R. (1987) Basic mechanisms of radiation effects in electronic materials and devices. Harry Diamond Laboratories, DHL-TR-2129.

McLean F. B., Boesch H. E. Jr and Oldham T. R. (1989) Electron–hole generation, transport and trapping in SiO_2. In *Ionizing Radiation Effects in MOS Devices and Circuits* (Edited by Ma T. P. and Dressendorfer P. V.), p. 87, Wiley, New York.

McLean F. B., Boesch H. E. Jr and McGarrity J. M. (1975) Hole transport and recovery characteristics of SiO_2 gate insulators. *IEEE Trans. Nucl. Sci.* **NS-23,** 1506.

McLean F. B., Boesch H. E. Jr and McGarrity J. M. (1978) Field-dependent hole transport in amorphous SiO_2. In *The Physics of SiO_2 and its Interfaces* (Edited by Pantelides S. T.), p. 19. Pergamon Press, New York.

McLean F. B., Ausmann G. A. Jr, Boesch H. E. Jr and McGarrity J. M. (1976) Application of stochastic hopping transport to hole conductance in amorphous SiO_2. *J. Appl. Phys.* **47,** 1529.

McWhorter P. J., Miller S. L. and Miller W. M. (1990) Modeling the anneal of radiation-induced trapped holes in a varying thermal environment. *IEEE Trans. Nucl. Sci.* **NS-37,** 1682.

Mikawa R. E. and Lenahan P. M. (1983) A comparison of ionizing radiation and hot-electron-effects in MOS structures. *IEEE Trans. Nucl. Sci.* **NS-31,** 1573.

Mikawa R. E. and Lenahan P. M. (1985) Structural damage at the Si/SiO_2 interface resulting from electron injection in metal–oxide semiconductor. *Appl. Phys. Lett.* **46,** 551.

Mikawa R. E. and Lenahan P. M. (1986) Electron spin resonance study of interface states induced by electron injection in metal–oxide semiconductor devices. *J. Appl. Phys.* **59,** 2054.

MIL HDBK 279 (1985) Total dose hardness assurance guidelines for semiconductor devices and microcircuits.

MIL-STD-883C, Method 1019.4. Steady state total dose irradiation procedure.

Montroll E. W. and Weis G. H. (1965) Random walks on lattices II. *J. Math. Phys. B.* **12,** 167.

Mott N. F. (1929) The scattering of fast electrons by atomic nuclei. *Proc. R. Soc. Lond.* **124A,** 425.

Mott N. F. (1932) The polarisation of electrons by double scattering. *Proc. R. Soc. Lond.* **135A,** 429.

Ning T. H. (1976) High-field capture of electrons by Coulomb-attractive centers in silicon dioxide. *J. Appl. Phys.* **47,** 3203.

Oldham T. R. (1982) Charge generation and recombination in silicon dioxide from heavy charged particles. Harry Diamond Laboratories Technical Report, HDL-TR-1985, Adelphi, MD.

Oldham T. R. (1985) Recombination along the tracks of heavy charged particles in SiO_2 films. *J. Appl. Phys.* **57,** 2695.

Oldham T. R. and McGarrity J. M. (1983) Comparison of

Co-60 response and 10 keV X-ray response in MOS capacitors. *IEEE Trans. Nucl. Sci.* **NS-30,** 4877.
Oldham T. R., Lelis A. J. Boesch H. E. Jr, Benedetto J. M., McLean F. B. and McGarrity J. M. (1987) Post-irradiation effects in field-oxide isolation structures. *IEEE Trans. Nucl. Sci.* **NS-34,** 1184.
Onsager L. (1934) Deviation from Ohm's law in weak electrolytes. *J. Chem. Phys.* **2,** 599.
Onsager L. (1938) Initial recombination of ions. *Phys. Rev.* **34,** 554.
Othmer S. and Srour J. R. (1980) Electron transport in SiO_2 films at low temperature. In *The Physics of MOS Insulators* (Edited by Lucovsky G., Pantelides S. T. and Galeener F. L.), p. 49. Pergamon Press, New York.
Pauling L. (1954) *J. Phys. Chem.* **58,** 662.
Pease R. L. and Alexander D. R. (1994) Hardness assurance for space system microelectronics. *Radiat. Phys. Chem.* **43,** 191.
Pease R., Emily D. and Boesch H. E. Jr (1985) Total dose induced hole trapping and interface state generation in bipolar recessed field oxides. *IEEE Trans. Nucl. Sci.* **NS-32,** 3946.
Pease R. L., Turfler R. M., Platteter D., Emily D. and Blice R. (1983) Total dose in recessed oxide digital bipolar microcircuits. *IEEE Trans. Nucl. Sci.* **NS-30,** 4216.
Poindexter E. H. and Caplan P. J. (1981) *EPR on MOS Interface States*, p. 150. INFOS, Springer, Berlin.
Poindexter E. H. and Caplan P. J. (1983) Characterization of Si/SiO_2 interfaces defects by electron spin resonance. *Prog. Surface Sci.* **14,** 201.
Powel R. J. and Berglund C. N. (1971) Photoinjection studies of charge distribution in oxide of MOS structures. *J. Appl. Phys.* **42,** 4390.
Revesz A. G. (1971) Defect structure and irradiation behavior of noncrystalline SiO_2. *IEEE Trans. Nucl. Sci.* **NS-18,** 113.
Revesz A. G. (1980a) The defect structures of vitreous SiO_2 films on silicon (I). *Phys. Stat. Sol.* **57,** 253.
Revesz A. G. (1980b) The defect structures of vitreous SiO_2 films on silicon (II). *Phys. Stat. Sol.* **57,** 637.
Revesz A. G. (1981) The defect structures of vitreous SiO_2. *Phys. Stat. Sol.* **58,** 107.
Saks N. S. and Brown D. B. (1989) Interface trap generation via the two-stage H^+ process. *IEEE Trans. Nucl. Sci.* **NS-36,** 1848.
Saks N. S. and Brown D. B. (1990) Observation of H^+ motion during interface trap formation. *IEEE Trans. Nucl. Sci.* **NS-37,** 1624.
Saks N. S., Klein R. B., Yoon S. and Griscom D. L. (1991) Formation of interface traps in metal–oxide-semiconductor devices during isochronal annealing after irradiation at 78 K. *J. Appl. Phys.* **70,** 3734.
Sakurai T. and Sugano T. (1981) Theory of continuously distributed trap states of $Si–SiO_2$ interfaces. *J. Appl. Phys.* **52,** 2889.
Scher H. and Lax M. (1973) Stochastic transport in a disordered solid I theory. *Phys. Rev. B.* **7,** 4491.
Scher H. and Montroll E. W. (1975) Anomalous transit time dispersion in amorphous solid. *Phys. Rev. B.* **12,** 2455.
Schrimpf R. V., Wahle P. J., Andrews R. C., Cooper D. B. and Galloway K. F. (1988) Dose-rate effects on the total-dose threshold-voltage shift of power MOSFETS. *IEEE Trans. Nucl. Sci.* **NS-35,** 1536.
Schwank J. R., Sexton F. W., Fleetwood D. M., Shaneyfelt M. R., Hughes K. L. and Rodgers M. S. (1989) Strategies for lot-acceptance testing using CMOS transistors and IC's. *IEEE Trans. Nucl. Sci.* **NS-36,** 1971.
Schwank J. R., Winokur P. S., McWhorter P. J., Sexton F. W., Dressendorfer P. V. and Turpin D. C. (1984) Physical mechanisms contributing to device rebound. *IEEE Trans. Nucl. Sci.* **NS-31,** 1434.
Schwank J. R., Sexton F. W., Fleetwood D. M., Jones R. V., Flores R. S., Rodgers M. S. and Hughes K. L. (1988) Temperature effects on the radiation response of MOS devices. *IEEE Trans. Nucl. Sci.* **NS-35,** 1432.
Schwerin A. v., Heyns M. M. and Weber W. (1990) Investigation on the oxide field dependence of hole trapping and interface state generation in SiO_2 layers using homogenenous nonavalanche injection holes. *J. Appl. Phys.* **67,** 7595.
Sexton F. W. and Schwank J. R. (1985) Correlation of radiation effects in transistors and integrated circuits. *IEEE Trans. Nucl. Sci.* **NS-32,** 3975.
Sigel G. H. Jr, Friebele E. J., Ginther R. J. and Griscom D. L. (1974) Effects of stochiometry on the radiation response of SiO_2. *IEEE Trans. Nucl. Sci.* **NS-21,** 56.
Simons M. and Hughes H. L. (1971) Short term charge annealing in electron-irradiated silicon dioxide. *IEEE Trans. Nucl. Sci.* **NS-18,** 106.
Simons M. and Hughes H. L. (1972) Determining the energy distribution of pulse-radiation-induced charge in MOS structures from rapid annealing measurements. *IEEE Trans. Nucl. Sci.* **NS-19,** 282.
Soppa W. M. and Wagemann H. G. (1980) Investigation and modelling of the surface mobility of MOSFET's from $-25°$ to $+150°C$. *IEEE Trans. Electron Devices* **35,** 970.
Srour J. R. (1983) Basic mechanisms of radiation effects on electronic materials, devices and integrated circuits. In *IEEE 1983 Nuclear and Space Radiation Effects Conference, Workshop*, p. 53.
Srour J. R., Curtis O. L. and Chiu K. Y. (1974) Charge transport studies in SiO_2: processing effects and implication for radiation hardening. *IEEE Trans. Nucl. Sci.* **NS-21,** 73.
Srour J. R., Hartmann R. A. and Kitazaki K. S. (1986) Permanent damage produced by single proton interaction in silicon devices. *IEEE Trans Nucl. Sci.* **NS-33,** 1597.
Summers G. P. (1992) Displacement damage: mechanisms and measurements. *IEEE Nuclear and Space Radiation Effects Conference Short Course*, New Orleans, LA.
Summers G. P., Burke E. A., Dale C. J., Wolicki E. A., Marshall P. W. and Gehlhausen M. A. (1987) Correlation of particle-induced displacement damage in silicon. *IEEE Trans. Nucl. Sci.* **34,** 1134.
Sun S. C. and Plummer J. D. (1980) Electron mobility in inversion and accumulation layers on thermally oxidized silicon surfaces. *IEEE Electron Devices* **ED-27,** 1497.
Svensson C. M. (1978) The defect of the $Si–SiO_2$ interface, a model based on trivalent silicon and its hydrogen "compounds". In *The Physics of SiO_2 and its Interfaces* (Edited by Pandalides S.), p. 328. Pergamon Press, New York.
Tzou J. J., Sun J. Y. C. and Sah C. T. (1983) Field dependence of two large hole capture cross sections in thermal oxide on silicon. *Appl. Phys. Lett.* **43,** 861.
Viswanathan C. R. and Maserjian J. (1976) Model of thickness dependence of radiation charging in MOS-structures. *IEEE Trans. Nucl. Sci.* **NS-23,** 1540.
Wall J. A. and Burke E. A. (1970) Gamma dose distribution at and near the interface of different materials. *IEEE Trans. Nucl. Sci.* **NS-17,** 305.
Warren W. L. and Lenahan P. M. (1986) Electron spin resonance study of high field stressing in metal–oxide–silicon devices. *Appl. Phys. Lett.* **49,** 1296.
Winokur P. S. and Boesch H. E. Jr (1981) Annealing of MOS capacitors with implications for the test procedures to determine radiation hardness. *IEEE Trans. Nucl. Sci.* **NS-32,** 4088.
Winokur P. S., Sexton F. W., Turpin G. L. and Turpin D. C. (1987) Total dose failure mechanisms of integrated circuits in laboratory and space environments. *IEEE Trans. Nucl. Sci.* **NS-34,** 1448.
Winokur P. S., Erret E. B., Fleetwood D. M., Dressendorfer P. V. and Turpin D. C. (1985) Optimizing and controlling

the radiation hardness of a Si-gate CMOS process. *IEEE Trans. Nucl. Sci.* **NS-32,** 3954.

Winokur P. S., Schwank J. R., McWhorter P. J., Dressendorfer P. V. and Turpin D. C. (1984) Correlating the radiation response of MOS capacitors and transistors. *IEEE Trans. Nucl. Sci.* **NS-31,** 1453.

Winokur P. S., Sexton F. W., Fleetwood D. M., Terry M. D., Shaneyfelt M. R., Dressendorfer V. P. and Schwank J. R. (1990) Implementing QML for radiation hardness assurance. *IEEE Trans. Nucl. Sci.* **NS-37,** 1794.

Winokur P. S., Sexton F. W., Schwank J. R., Fleetwood D. M., Dressendorfer P. V., Wrobel F. and Turpin D. C. (1986) Total-dose radiation and annealing studies: Implication for hardness assurance testing. *IEEE Trans. Nucl. Sci.* **NS-33,** 1343.

Wood M. H. and Williams R. (1976) Hole traps in silicon dioxide. *J. Appl. Phys.* **47,** 1082.

Wulf F., Boden A. and Bräunig D. (1990) Total dose study on LS-, ALS-, and F-technology integrated circuits. In *Proc. ESA Electronic Components Conference*, ESTEC Noordwijk, ESA SP-313, p. 407.

Wulf F, Bräunig D. and Boden A. (1981–1990) *GfW-Handbook for Data Compilation of Irradiation Tested Electronic Components: Hahn-Meitner-Institut Berlin, test report HMI-B248*, Vol. 1–6.

Young D. R., Erene E. A., Di Maria D. J., De Keersmaeker R. F. and Massond H. Z. (1979) Electron trapping in SiO_2 at 295 and 77 K. *J. Appl. Phys.* **50,** 6366.

Zekeriya V. and Ma T. P. (1984a) Dependence of X-ray generation of interface traps on gate metal induced interfacial stress in MOS structures. *IEEE Trans. Nucl. Sci.* **NS-31,** 1261.

Zekeriya V. and Ma T. P. (1984b) Dependence of radiation-induced interface traps on gate Al thickness in metal/SiO_2/Si structures. *J. Appl. Phys.* **56,** 1017.

Zekeriya V. and Ma T. P. (1984c) Effect of stress relaxation on the generation of radiation-induced interface traps in post-metal-annealed Al–SiO_2–Si devices. *Appl. Phys. Lett.* **45,** 249.

Zupac D., Galloway K. F., Schrimpf R. D. and Augier P. (1992) Effects of radiation-induced oxide-trapped charge on inversion-layer hole mobility at 300 and 77 K. *Appl. Phys. Lett.* **60,** 3156.

Ziegler J. F., Biersack J. P. and Witmark U. (1985) *The Stopping and Range of Ions in Solids.* Pergamon Press, New York.